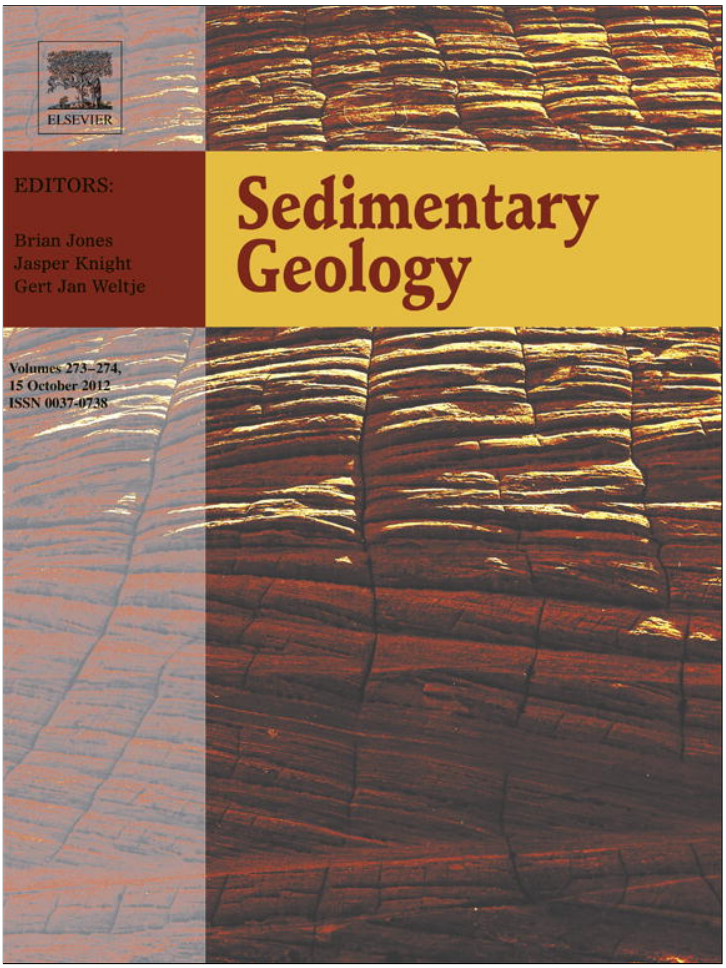

Sedimentary Geology 273–274 (2012) 73–90

Contents lists available at SciVerse ScienceDirect

Sedimentary Geology

journal homepage: www.elsevier.com/locate/sedgeo

Carbonate facies of the Upper Triassic Ojo Huelos Member, San Pedro Arroyo Formation (Chinle Group), southern New Mexico: Paleoclimatic implications

Lawrence H. Tanner [a,*], Spencer G. Lucas [b]

[a] Department of Biological Sciences, Le Moyne College, Syracuse, NY 13214 USA
[b] New Mexico Museum of Natural History, 1801 Mountain Road N.W., Albuquerque, NM 87014, USA

ARTICLE INFO

Article history:
Received 17 May 2012
Received in revised form 3 July 2012
Accepted 4 July 2012
Available online 14 July 2012

Editor: B. Jones

Keywords:
Lacustrine
Palustrine
Pedogenesis
Calcrete
Chinle Group
Adamanian

ABSTRACT

The Upper Triassic (Adamanian LVF) Ojo Huelos Member of the San Pedro Arroyo Formation (Chinle Group) is a distinctive, carbonate-rich unit that occurs in the lower Chinle section of central New Mexico. The member consists mainly of micritic lime mudstones, ostracodal wackestones to grainstones, peloidal grainstones and distinctive pisolitic rudstones, interbedded with fine-grained siliciclastic mudstones. Most limestones exhibit some evidence of pedogenic brecciation and root penetration, and porous fabrics similar to those of modern limestone tufas occur locally. The interbedded mudstones are typically lenticular and commonly display a blocky ped fabric in which subequant peds are separated by sparry calcite veins. Fossils from the Ojo Huelos Member are freshwater (darwinulid) ostracodes, various freshwater fishes and aquatic/amphibious tetrapods–metoposaurs and phytosaurs. We interpret the carbonate facies as the deposits of carbonate lakes, ponds and wetlands that were partly spring-fed, whereas the interbedded and surrounding mudstones were alluvial in origin. The groundwater and overland hydrology of the region was likely controlled by the relative proximity to an upland recharge area in the Mogollon Highlands to the south, but sedimentary fabrics record strong overprinting by desiccation and pedogenic reworking. Consequently, we interpret the Ojo Huelos Member as recording a climate that varied from subhumid to semi-arid, which caused episodic falls in the hydrologic base-level. This resulted in landscape degradation, exemplified by significant pedogenic and erosional reworking of the carbonate sediments and fluvial incision.

1. Introduction

Interest in the sedimentology of the Upper Triassic Chinle Group deposits stems in part from recognition of the paleoclimatic archives contained therein (e.g., Parrish, 1993; Dubiel, 1994; Tanner, 2000; Tanner and Lucas, 2006; Cleveland et al., 2008a, 2008b). Indeed, sedimentary records of Late Triassic paleoclimate are particularly valuable for their potential to resolve questions of environmental change coincident with the great biotic decline of this time interval; aridification of the Pangean interior and intense warming due to the eruptions of the flood basalts of the Central Atlantic magmatic province (CAMP) have been oft-cited as factors that contributed to decreasing biotic diversity in both continental and marine realms (Colbert, 1958; Tucker and Benton, 1982; Simms and Ruffell, 1990; Tanner, 2000; Tanner et al., 2001, 2004).

Tanner (2000, 2003) and Tanner and Lucas (2006) surveyed the sedimentary facies and pedogenic features in the formations of the Chinle Group and concluded from this evidence that the climate on the Colorado Plateau was drier during the Norian–Rhaetian than during the Carnian, supporting the earlier interpretation of Blakey and Gubitosa (1984). Notably, this interpretation was contrary to that of Dubiel et al. (1991) and Parrish (1993), who interpreted the same sedimentary evidence as indicating a moist climate until the very end of the Triassic, or at least through the end of the Norian. Overall, the deposition of Upper Triassic sediments indicating increasing aridity coincides with the breakup of Pangaea and the northward drift of North America (Dubiel et al., 1991; Parrish, 1993; Olsen, 1997; Clemmensen et al., 1998; Kent and Tauxe, 2005).

The importance of the paleoclimatic interpretation of the Ojo Huelos Member of the San Pedro Arroyo Formation, a distinctive carbonate-rich unit that crops out in central New Mexico (Figs. 1–2), derives from its stratigraphic position relative to other Chinle Group formations for which paleoclimate information is available. The San Pedro Arroyo Formation is underlain by alluvial strata of the Shinarump Formation, which display features suggesting deposition during subhumid conditions (Dubiel et al., 1991; Parrish, 1993; Dubiel, 1994; Tanner and Lucas, 2007). Although Upper Triassic strata overlying the San Pedro Arroyo Formation are not preserved in central New Mexico, strata that occupy that stratigraphic position elsewhere (the Petrified Forest and Owl Rock formations) exhibit features, such as a predominance of Aridisol-type paleosols (cf. Tanner and Lucas, 2006), that suggest a transition to a semi-arid paleoclimate. Consequently, the San Pedro Arroyo Formation occupies an important position with

* Corresponding author.
E-mail address: tannerlh@lemoyne.edu (L.H. Tanner).

0037-0738/$ – see front matter © 2012 Elsevier B.V. All rights reserved.
doi:10.1016/j.sedgeo.2012.07.001

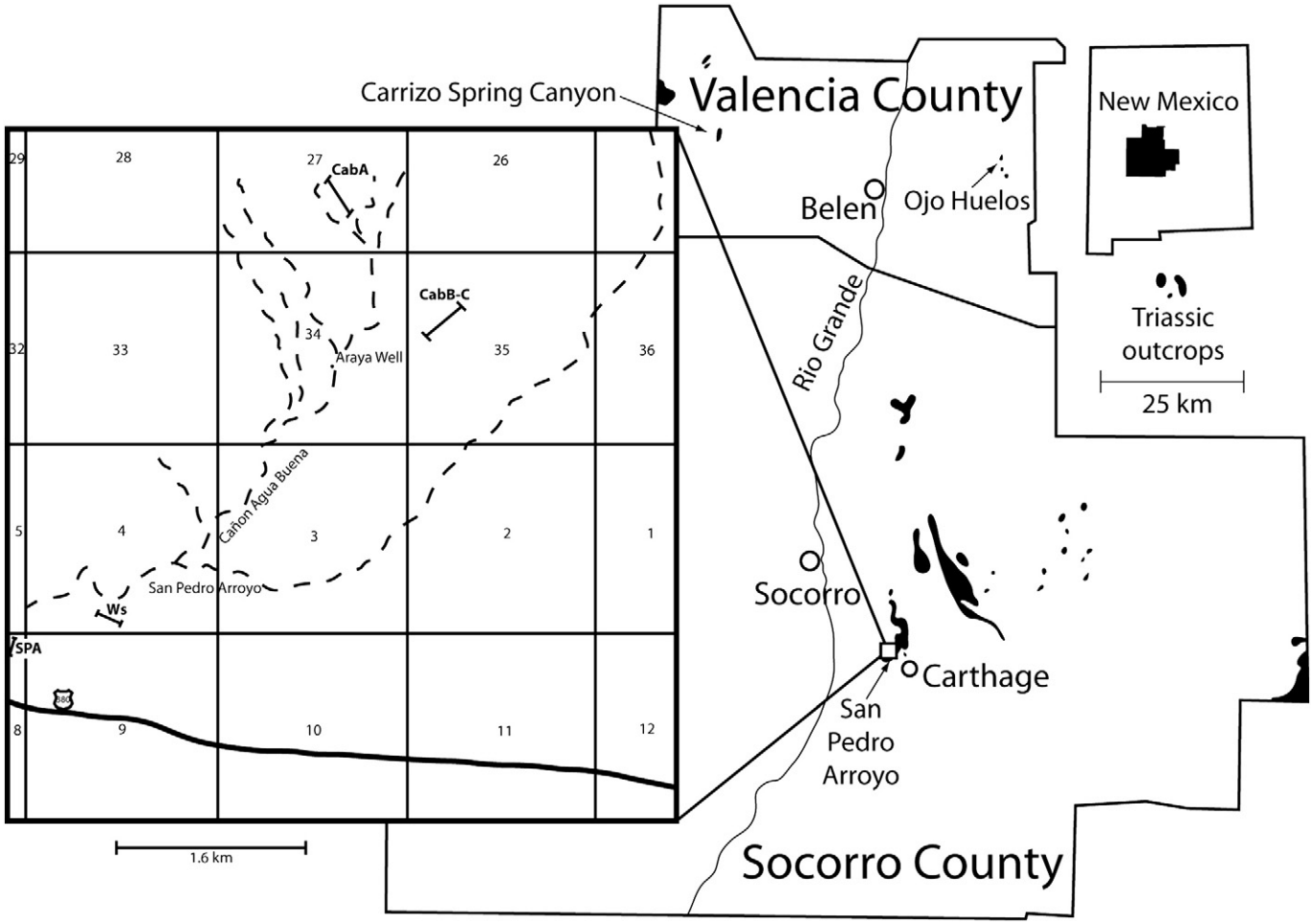

Fig. 1. Location map of the study area in central New Mexico, western U.S.A, showing locations of measured sections (modified from Spielmann and Lucas, 2009). Locality abbreviations on detailed map of San Pedro Arroyo area are: CabA = Cañon Agua Buena A, CabB-C = Cañon Agua Buena B–C, SPA = San Pedro Arroyo and W = Weber.

regard to the interpretation of the evolution of Late Triassic paleoclimate in the American Southwest.

2. Regional setting and stratigraphy

The field location for this study, in south-central New Mexico (Fig. 1), lies within the Rio Grande rift, a north–south chain of. fault-bounded basins formed by late Cenozoic crustal extension. This area was located at substantially lower latitudes during Late Triassic time than at present (Scotese, 1994; Molina-Garza et al., 1995; Kent and Olsen, 1997, 2000), possibly drifting from a near-equatorial to a sub-tropical position during the Late Triassic (Kent and Tauxe, 2005).

Deposition of Chinle Group strata occurred in a continental back-arc basin (the Chinle basin) that extended from southwestern Texas to northern Wyoming (Lawton, 1994; Lucas et al., 1997). Chinle strata are separated in most places from the underlying Moenkopi Formation/Group by a regional unconformity, which formed an incised surface on which Chinle strata were deposited. Streamflow across the landscape was primarily to the northwest, mainly from the Mogollon highlands, approximately 200 km to the south and southwest. Deposition of the Shinarump and San Pedro Arroyo formations, and lateral equivalents, was controlled by the paleotopography of the Tr-3 unconformity surface (Blakey and Gubitosa, 1983, 1984; Demko et al., 1998), burying the erosional topography of the unconformity (Lucas, 1991; Lucas et al., 1997, 2004; Spielmann and Lucas, 2009).

Lucas (1991) used the lithologic and stratigraphic similarities of the Triassic strata of Socorro and Valencia counties, central New Mexico, to the Triassic strata of the nearby Chama basin and Colorado Plateau to identify the Middle Triassic Moenkopi Formation and the Upper Triassic Shinarump and San Pedro Arroyo formations of the Chinle Group (Lucas et al., 2004; Spielmann and Lucas, 2009) (Fig. 2). The San Pedro Arroyo Formation was named by Lucas (1991) to encompass strata overlying basal Chinle strata, i.e., the Shinarump Formation, with the type section at San Pedro Arroyo in Socorro County (Fig. 1).

The Ojo Huelos Member is a laterally persistent, carbonate-rich unit within the mainly siliciclastic sediments of the San Pedro Arroyo Formation that forms a persistent, distinctive marker unit throughout the Upper Triassic section in both Valencia and Socorro counties, from Hubbell Springs near Belen and Carrizo Arroyo in the Lucero uplift to its southernmost outcrop near Carthage (Lucas, 1991; Lucas et al., 2004; Cather and Osburn, 2007) (Fig. 1–2). Lucas (1991) named the unit and established the type section in southern Valencia County at Ojo Huelos (Lucas, 1991; Lucas et al., 2004) (Fig. 1). The base of the Ojo Huelos Member is the lowest limestone bed above the Araya Well Member. Spielmann and Lucas (2009) reported 16.5 m as the maximum thickness of the unit across its outcrop belt. The overlying mudstone-dominated strata are the Cañon Agua Blanca Member (Spielmann and Lucas, 2009).

The age of the San Pedro Arroyo Formation strata is provided most reliably by a vertebrate fossil fauna that indicates an Adamanian (mid-Late Triassic) age, though it is possible that the upper part of the San Pedro Arroyo Member is as young as Revueltian (Case,

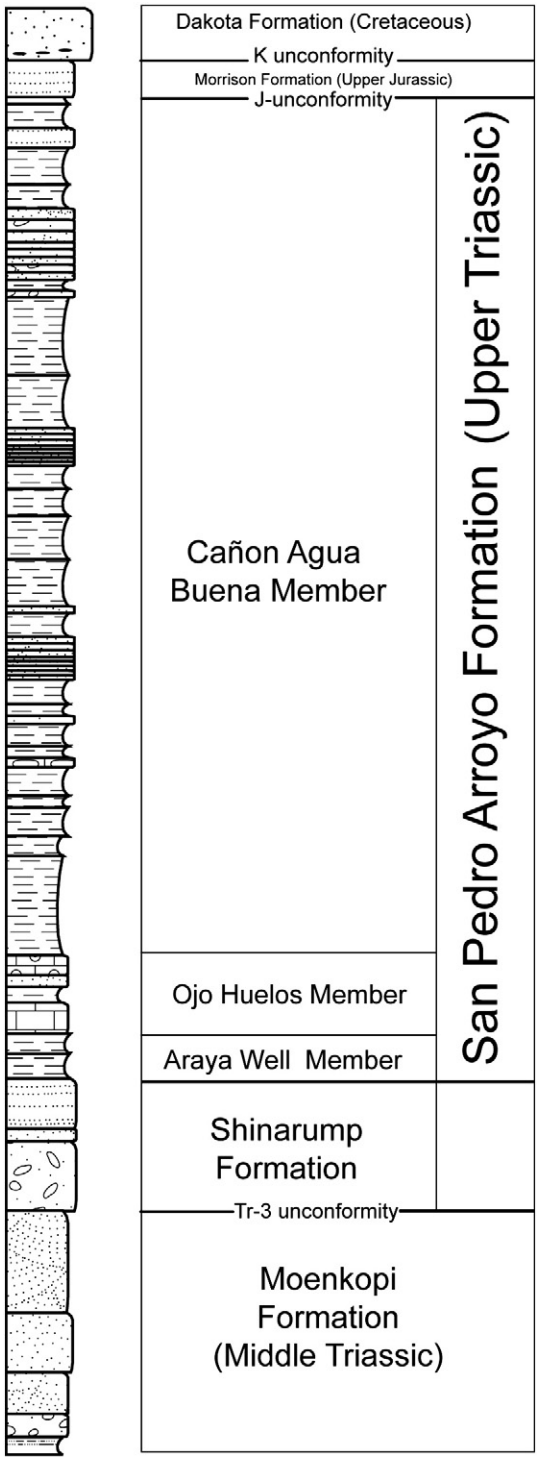

Fig. 2. Generalized lithostratigraphy of the Upper Triassic Chinle Group section in Valencia and Socorro Counties, New Mexico, showing stratigraphic context of the Ojo Huelos Member.

1916; Lucas, 1991; Lucas and Heckert, 1994; Heckert, 1997, 2004; Heckert and Lucas, 2002a; Spielmann and Lucas, 2009). Thus, deposition of the Ojo Huelos Member took place either during the latest Carnian stage, if a "short Norian" is accepted (Lucas et al., 2007; Heckert et al., 2009; Lucas, 2010), or early to middle Norian, if the "long Norian" is invoked (cf. Irmis et al, 2010; see discussion in Lucas et al., 2012). The Ojo Huelos Member itself yields a particularly rich fossil fauna that includes darwinulid ostracodes, semionotid and redfieldiid fish, the hybodont shark *Lissodus*, and fragmentary bones of metoposaurid amphibians, phytosaurs and indeterminate reptiles (Lucas, 1991; Heckert and Lucas, 2002a; Heckert et al., 2007).

3. Methods

In addition to field description, the lithofacies described below were sampled for petrographic and geochemical analyses. Microscopic features were examined on standard thickness (30 μm) petrographic thin sections. The mineralogy of framework grains and cements was determined by X-ray diffraction analysis of random powder mounts and of clays via oriented mounts using a Bruker D2 Phaser diffractometer with a Cu-anode X-ray tube operating at 30 kV and 10 mA. All carbonates in the Ojo Huelos Member are identified as low-Mg calcite. Carbonate and clay microfabrics were studied by scanning electron microscopy using a JEOL JSM 6510-LV microscope on gold-coated specimens at an accelerating voltage of 20 kV under high vacuum conditions.

4. Field observations

The lower part of the San Pedro Arroyo Formation, the Ojo Huelos Member in particular, was examined in detail at eight outcrop sections at five separate locations along washes and on hillsides in southern New Mexico (Fig. 1). At all of the sites examined in this study, the base of the outcrop exposure includes reddish sandstones and mudstones assignable to the underlying Moenkopi Formation. In most sections, these are overlain (disconformably) by conglomerates and conglomeratic sandstones comprising varying proportions of intrabasinal clasts, of mudstone and limestone, and extrabasinal material (mainly chert), assignable to the Shinarump Formation. These are in turn overlain by the mudstones of the lower San Pedro Arroyo Formation.

4.1. Ojo Huelos

The type location for the Ojo Huelos Member is a hillside exposure of ~10 m thickness located 20 km east of the town of Belen in Valencia County (Fig. 1). The Shinarump Formation is not clearly exposed here, but its position can be approximated by the occurrence of abundant extra-basinal (siliceous) clasts at a discrete level on the slope (Fig. 3). The lowermost unit that can be definitively assigned to the Ojo Huelos Member is a 0.5-m thick bed of brownish-yellow, mottled to porous limestone (Fig. 4A). The overlying section comprises beds of gray ostracodal limestone with fabrics varying from wackestone to grainstone. Slope-forming, yellowish-green claystone separates these limestones from the overlying beds of ostracodal limestone, locally containing abundant fish scales and bones (Heckert and Lucas, 2002a; Heckert et al., 2007), and cm-scale pisoids at the top. Covered slope underlies the uppermost carbonate bed, which consists of rooted, nodular-weathering, micritic limestone (Fig. 4B).

4.2. Cañon Agua Blanca

The thickest section of the Ojo Huelos Member was measured at Cañon Agua Blanca, in Socorro County, where exposures occur in three closely-spaced sections in ravines, each separated by several hundred meters (Fig. 1). The most complete of these totals ~40 m in thickness and consists mainly of cross-bedded sandstones, massive to brecciated micritic limestone, pisolitic rudstone and mudstones (Fig. 3). The base of the Ojo Huelos Member here is unique in consisting of distinctive meter-scale beds composed almost entirely of pisolitic rudstone (Fig. 5A). Bedding varies from massive to crudely stratified, to tabular sets. Some beds display an upward-decreasing size of the pisoids and are capped by litharenite sandstone completely lacking pisoids. Finer-grained pisolitic beds contain a greater proportion of matrix and a wider range of clast sizes, including smaller, irregularly-shaped carbonate clasts, petrified wood and fossil bones

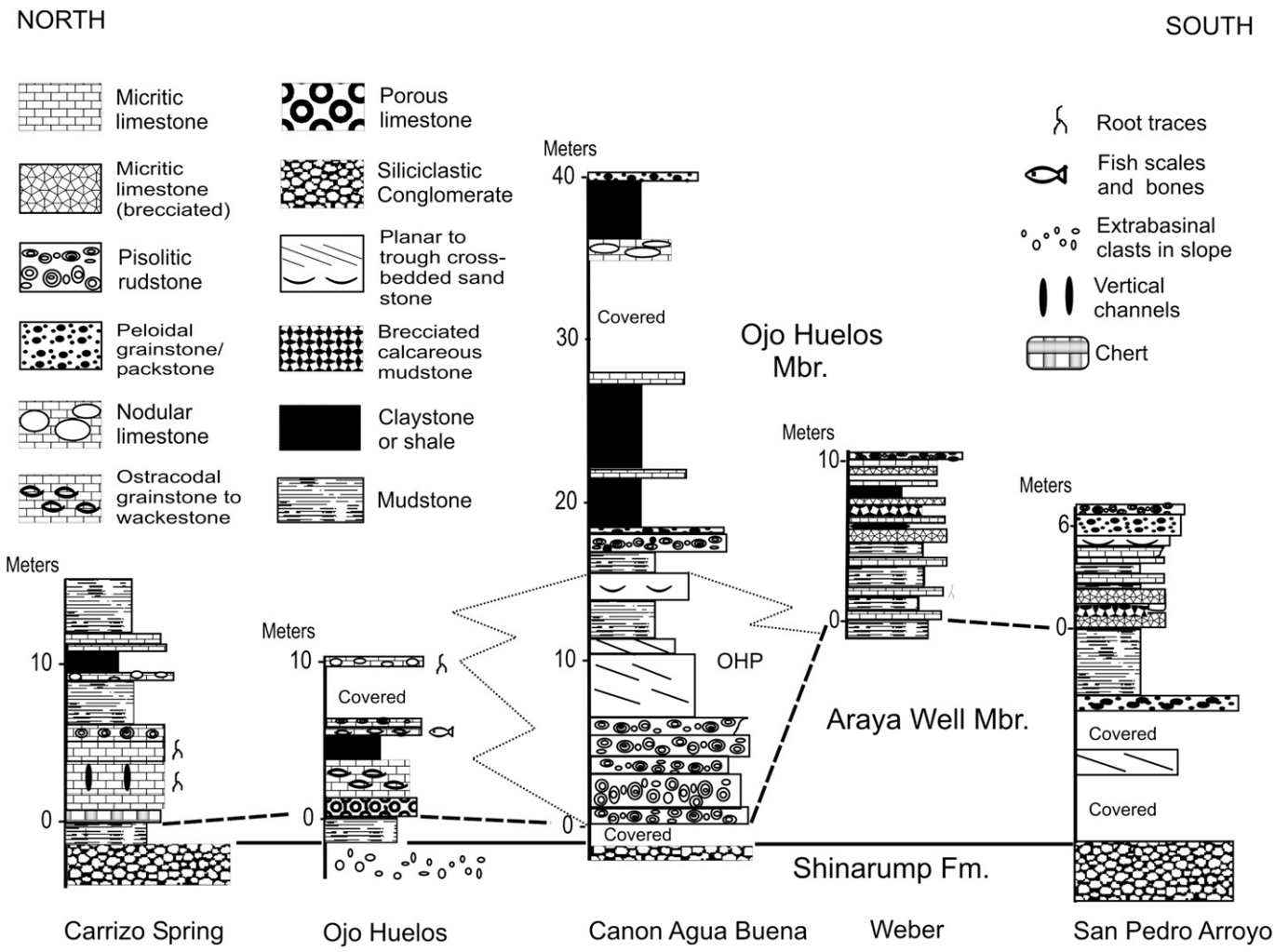

Fig. 3. Measured sections for all of the study sites described in the text. No horizontal scale is implied; see Fig. 1 for distances between locations. Lithologies shown here are described in detail in the text and presented in Table 1. The datum shown is the top of the Shinarump Formation. The base of the Ojo Huelos Member is marked at 0 m in each column. OHP refers to the Ojo Huelos Paleovalley, an inferred stream valley incised into the lacustrine and alluvial carbonate and siliciclastic sediments of the Ojo Huelos Member (see also Fig. 16).

up to 6 cm long, likely representing metoposaurid amphibians (Fig. 5B). The overlying strata consist of tabular sets of planar cross-bedded sandstone (Fig. 5C) and lenticular beds of trough cross-bedded sandstone interbedded with slope-forming mudstone. The sandstone-mudstone is overlain by unstratified, pisolitic grainstone to peloidal packstone comprising a mixture of pisoids up to 2 cm in diameter and gray to white, micritic limestone and red mudstone clasts of similar size (Fig. 5D). The remainder of the exposed section consists of greenish-gray to reddish-purple claystone interbedded with thin beds of mottled, micritic limestone that are nodular weathering and locally cherty.

Two other sections were measured at Cañon Agua Buena, each offset successively to the southwest by 100 m to 200 m. Although the exposure in the secondary sections is not as complete as in the primary section described above, the lithologies and their relative stratigraphic order are broadly correlative, with some striking differences. In particular, at the stratigraphic level of the pisolites in sections A and B, section C instead displays peloidal limestones, and at the level of

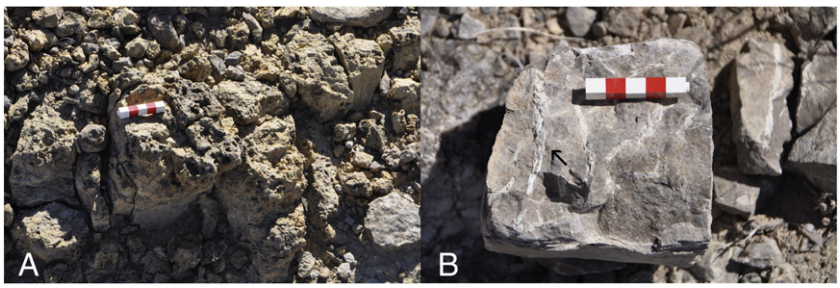

Fig. 4. Features of the section at Ojo Huelos. A. The basal limestone is yellowish-brown, porous (vuggy) and rests on calcareous mudstone. Divisions on scale are 1 cm. B. Limestones near the top of the section are micritic and contain branching, clay-filled root traces (arrow).

Fig. 5. Features of the section measured at Cañon Agua Blanca. A. Basal unit of the Ojo Huelos Member is pisolitic rudstone. Individual pisoids are 2 cm to 3 cm wide. Hammer is 30 cm long. B. Large metoposaurid amphibian bone fragment in pisolitic rudstone. Scale = 5 cm. C. Beds of planar cross-bedded litharenite sandstone that occur between pisolitic beds. Section shown is about 2.7 m thick. D. Upper pisolitic beds are a conglomerate of pisoids, red mudstone clasts and pale gray clasts of micritic limestone.

the pisolite unit above the sandstone in section A (also present in section B), section C instead displays grayish-red to greenish mottled, nodular limestone.

4.3. San Pedro Arroyo

The type section for the San Pedro Arroyo Formation is located 23 km SE of the city of Socorro, Socorro County (Fig. 1). The 8-m section Ojo Huelos Member is well-exposed on a hillside that overlooks the arroyo (Fig. 3). Covered slope separates the Shinarump conglomerates from the interbedded limestone and siliciclastic beds that constitute the exposed Ojo Huelos Member in this section. The limestones are decimeter-scale beds of nonfossiliferous micrite, color-mottled gray to reddish-brown and massive to brecciated (Fig. 6A). Individual beds are commonly lenticular in shape and have irregular bases (Fig. 6B). The interbedded mudstones are brown to green to mottled purple-green, and are lenticular to laterally continuous over the outcrop face (approximately 100 m). The grain size of the mudstone varies from fine to sandy, but is typically calcareous. Drab root traces up to 5 cm long are common in the brown, sandy mudstones. Commonly, these mudstones have a brecciated fabric and contain thin calcite veins (Fig. 6C).

4.4. Weber

The Weber section is located 2 km ENE of the San Pedro Arroyo locale (Fig. 1), so it provides an excellent point for comparison of the lateral continuity of the lithofacies observed at the latter site. The 10-m section is exposed along the banks and in the bed of a shallow wash. The Ojo Huelos Member consists of decimeter-scale, micritic limestone beds that are mostly mottled brown-gray and commonly display a brecciated fabric. Drab-colored root traces occur in several

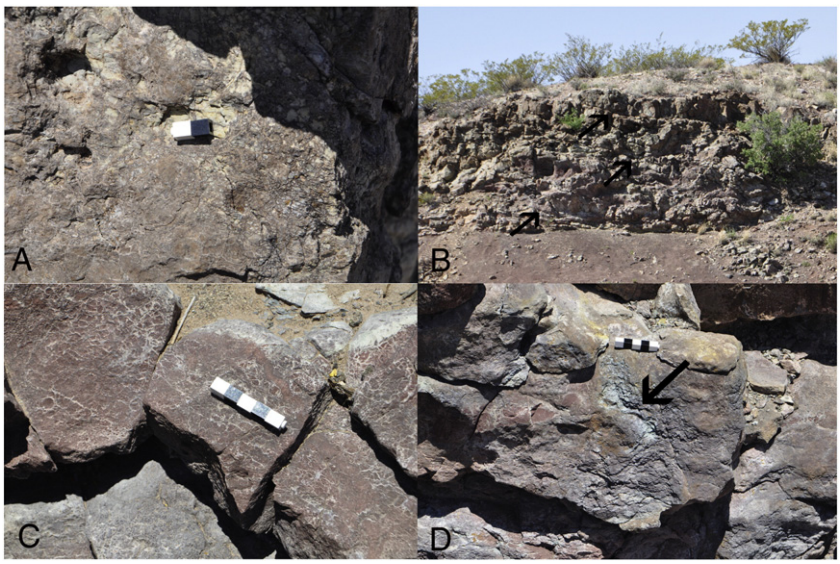

Fig. 6. Features of sections at San Pedro Arroyo and Weber. A. Plan view of the top of a limestone bed at San Pedro Arroyo displays brecciated fabric and microkarst topography. Scale bar = 2 cm. B. Limestone beds of the Ojo Huelos Member are lenticular in shape and typically display sharp, irregular bases (indicated by arrows). C. Mudstone with brecciated fabric exhibits angular mudstone blocks forming a nearly interlocking, or jig-saw fabric. Scale bar = 5 cm. D. Drab root trace (arrow) penetrating limestone bed at Weber.

of the limestone beds (Fig. 6D). The uppermost bed is a pisolitic rudstone. Mudstones in the Ojo Huelos strata include coarse, calcareous, slope-forming red to mottled mudstones as well as discrete beds of greenish claystone to dark reddish-brown mudstone. The thickest mudstone bed has a pervasively brecciated fabric with calcite veins, similar to the mudstones seen in the San Pedro Arroyo section.

4.5. Carrizo Spring

The northernmost exposure of the Ojo Huelos Formation occurs at Carrizo Spring, where uplifted and tilted strata of the Moenkopi Formation and Chinle Group are well-exposed along either side of Carrizo Spring Canyon (Lucas et al., 2004), 32 km west of the town of Los Lunas, Valencia County (Fig. 1). The lowermost micritic limestone unit is distinct from limestones at other outcrop locations in that the lower part of the unit locally displays crude, wavy color-banding – alternating white, tan and brownish-orange layers (Fig. 7A). These white and orange bands are siliceous and locally are porous. Sub-vertical to sub-horizontal, mudstone-filled channels, up to 20 cm long and downward-branching, occur locally and most prominently near the top of the lower bed. The upper bed also consists of micritic limestone, locally nodular weathering. The bed is pervasively penetrated by vertical, mudstone-filled channels, which are concentrated in the lower 1.0 m (Fig. 7B). Mudstone-filled channels also occur in the uppermost part of the bed, extending downward from the top of the bed, but they are less common and smaller than below. The top of the bed is nodular weathering and contains crude pisoids.

The overlying strata consist of interbedded micritic to nodular limestones and slope-forming mudstones.

5. Lithofacies analysis

The strata that comprise the Ojo Huelos Member at the locations described above can be characterized as eight distinct lithofacies that are distinguished by both their sedimentologic and petrographic characteristics, as described below and in Table 1.

5.1. Micritic (nonfossiliferous) limestones

5.1.1. Observations

Dense, micritic limestone occurs in all sections in beds ranging from 0.2 to 1.1 m thick. Most beds have a lightly mottled appearance, varying from red-green to grayish-purple-green to tan-gray. A vaguely to prominently brecciated fabric throughout all or part of the bed is the most consistent characteristic of this facies (Fig. 8A). This fabric comprises angular domains of micrite up to 10 cm in diameter, although the domain boundaries vary from sharp to diffuse (Fig. 8B, C), separated by millimeter-wide to centimeter-wide veins of equant crystals of microspar to sparry calcite; spherulitic chalcedony is rare. In some places, the domains consist of fine, dense micrite that is intensely brecciated on a sub-mm scale to form 0.2 to 2 mm clasts separated by sparry veins. In other places, the clasts display an undifferentiated massive to (less-common) clotted-peloidal fabric with circumgranular cracking, comprising micrite that is silty to slightly argillaceous (Fig. 8D). The veins between micritic domains are curved to straight, have vertical to horizontal orientations, and are filled variously by (most commonly) nonluminescent sparry calcite or calcite- to chert-cemented siltstone.

Subvertical channels interpreted as root traces commonly extend from the upper contact of beds and taper downward and bifurcate. These comprise millimeter-scale, drab-gray filaments to fissures up to 40 cm long and 6 cm wide (Fig. 8E). They are filled variously by fine to coarse calcite spar, as well as peloids, silt, clay, chert, and spherultic chalcedony. Subhorizontal, nontapering cyclindrical burrows are 0.5 to 1.0 cm wide and up to 5 cm long. Beds commonly display an irregular upper surface capped by a thin (1 mm to 3 mm) veneer of massive micrite. Wavy lamination distinguishes the lowermost limestone bed at Carrizo Spring, but much of the original host rock has been replaced by chert, rendering the origin of the lamination (i.e., primary v. diagenetic artifact; cf. Bustillo, 2010) problematic.

5.1.2. Interpretation

The primary sedimentary fabric in this facies is massive micritic carbonate consisting of subhedral calcite crystallites from 0.4 to 2 μm (Fig. 8F). Although body fossils and charophyte debris are generally lacking, the sedimentary texture suggests a lacustrine depositional setting (Kelts and Hsü, 1978). The lack of sedimentary structures in lacustrine carbonate commonly is attributed to extensive bioturbation in well-oxidized waters (Gierlowski-Kordesch, 2010), although several authors have commented that a uniform micritic fabric might result

Table 1
Summary of lithofacies characteristics and interpretations.

Lithofacies	Characteristics	Interpretation
Micritic limestone	Nonfossiliferous Uniform to mottled Faint to pronounced brecciation	Lacustrine to palustrine
Ostracodal limestone	Wackestone to grainstone Micritic	Perennial lacustrine
Porous limestone	Irregular mm-scale pores to vertically elongated and cylindrical vugs Ostracode-bearing	Spring tufa deposit
Peloidal grainstone/wackestone	Well sorted Well-rounded micritic grains Sandy matrix	Reworked palustrine deposited by stream flow
Pisolitic rudstone	cm-scale pisoids Tabular beds fining-upward	Pedogenic origin of pisoids Alluvial deposition
Nodular limestone	cm-scale micritic nodules Argillaceous to sandy/pebbly matrix	Stages II to III calcrete
Brecciated mudstone	Mudstone blocks separated by calcite veins Jig-saw fabric	Desiccated alluvial mud
Litharenite sandstone	Tabular sets Planar to trough cross-beds	Stream bar and dune deposits

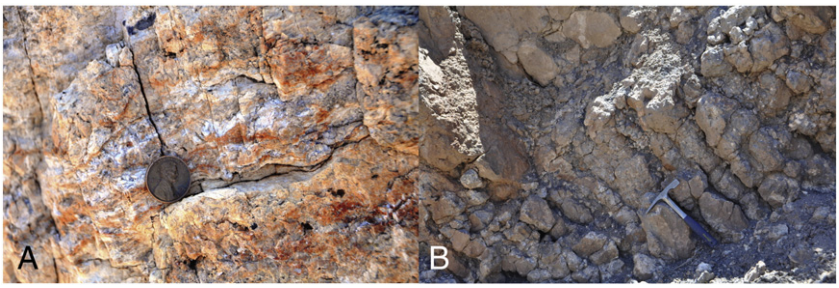

Fig. 7. Features of the section at Carrizo Spring Canyon. A. The lower bed of the basal limestone unit is locally porous and displays laterally discontinuous orange-white banding that is partially siliceous. B. The lower part of the upper limestone bed displays prominent vertical channels, typically 0.6 m to 0.7 m long, locally filled by gray mudstone.

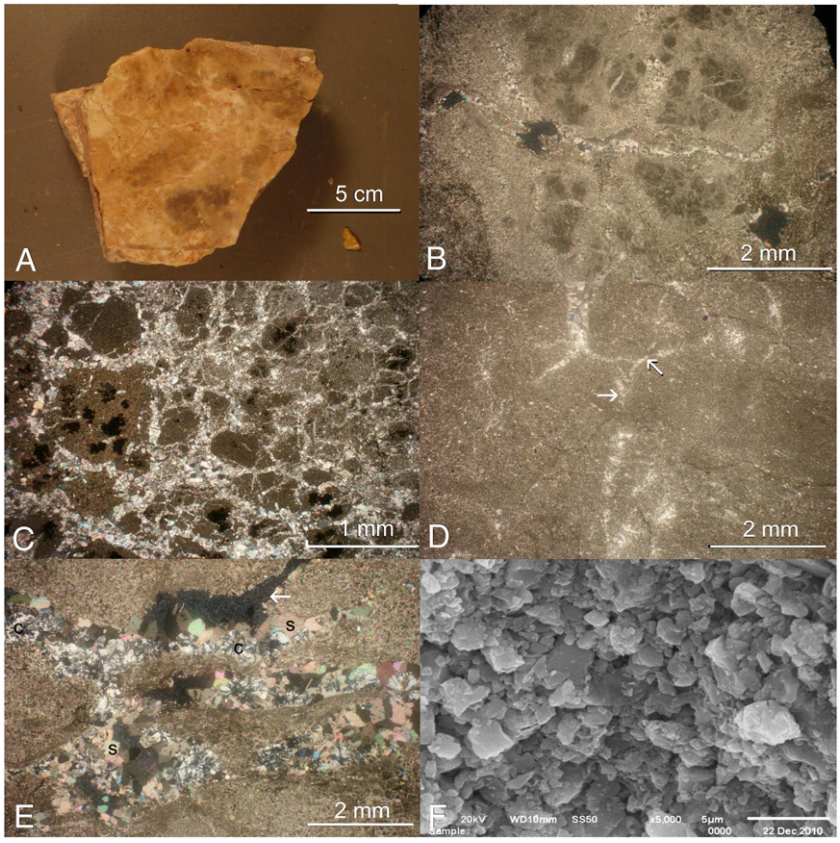

Fig. 8. Features of micritic limestone lithofacies. A. Sample of micritic limestone from Carrizo Spring displays a brecciated fabric. B. Sample of brecciated limestone from Carrizo Spring exhibits domains with dense micritic centers and diffuse boundaries, separated by veins of calcite spar. C. Sample of brecciated limestone from Carrizo Spring in which the micrite domains have very sharp boundaries separated by calcite spar. D. Micritic limestone from San Pedro Arroyo with incipient brecciation, characterized by clotted peloidal fabric and circumgranular cracking (arrows). E. Channel within micritic limestone from Carrizo Spring, presumably formed by root penetration, is filled by a combination of calcite spar (s), chalcedony (c) and detrital chloritic clay (arrow). F. SEM micrograph of micritic limestone from Ojo Huelos site showing range of crystallite sizes.

instead from rapid sedimentation (Verrechia, 2007; Alonso-Zarza et al., 2011). In the Ojo Huelos Member, however, the variability of bed thickness, limited lateral extent of the facies, interbedding with fine-grained siliciclastic sediments and evidence of pedogenesis suggests that much of the deposition took place in shallow carbonate ponds and wetlands subject to episodic desiccation, rather than large, open lacustrine water bodies (Platt and Wright, 1991; Alonso-Zarza et al., 1992; Armenteros et al., 1997; Alonso-Zarza and Wright, 2010a). Nevertheless, the lack of evaporites indicates that the water in these lakes and ponds was only rarely saline.

The brecciated to clotted peloidal fabric, color mottling (or pseudogley), and circumgranular cracking reflect minor pedogenic modification of the original carbonate textures by repeated desiccation during episodes of water table decline and water body shrinkage, during which plant roots penetrated the sediment (Plaziat and Freytet, 1978; Platt, 1989, 1992; Freytet and Verrecchia, 2002; Alonso-Zarza, 2003; Alonso-Zarza and Wright, 2010a). Subsequent phreatic cementation filled the desiccation and circumgranular cracks with sparry cement.

Brecciated and peloidal fabrics with circumgranular cracks and mottling are common features of palustrine sediments (Plaziat and Freytet, 1978; Platt, 1989, 1992; Platt and Wright, 1992; Armenteros et al., 1997; Freytet and Verrecchia, 2002; Alonso-Zarza, 2003; Alonso-Zarza and Wright, 2010a), suggesting a palustrine origin for these fabrics in the Ojo Huelos carbonates. Tanner (2000) similarly interpreted carbonate fabrics in the (Norian) Owl Rock Formation of the upper Chinle Group that resemble those of the Ojo Huelos Member, as lacustrine/palustrine deposits. The clast domains in the Ojo Huelos brecciated facies formed by desiccation cracking and root penetration of the original sediments, resulting from shrinkage cracking during periods of emergence, typically under semiarid conditions (Platt and Wright, 1992; Armenteros et al., 1997). Color mottling resulted from remobilization of Fe oxides and hydroxides during conditions of fluctuating water table or Eh and pH (Plaziat and Freytet, 1978; Platt, 1989). Some beds (e.g., the sections at Carrizo Arroyo and Ojo Huelos) exhibit nearly vertical, downward-tapering channels or fissures that were likely created by root penetration and solution enlargement, indicating extensive subaerial exposure (Platt, 1989). Irregular upper bed boundaries that locally have up to 10 cm of relief typically display a thin micritic veneer overlying a brecciated zone, and may have formed by incipient karstification.

The micritic to brecciated limestone facies is interbedded and gradational with the other facies described below and represents deposition mainly in shallow perennial to ephemeral lakes and ponds occupying topographic lows on a broad floodplain. The less disrupted limestones were deposited in the deeper areas of these shallow bodies but were still subjected to episodic exposure during lake regression (Alonso-Zarza and Wright, 2010a). The laterally equivalent, more intensely brecciated facies represents the low-gradient margins of lakes or laterally equivalent wetlands that were subject to thorough pedogenic reworking during periods of groundwater lowstand when desiccation shrinkage and root penetration caused brecciation (see Fig. 3, Alonso-Zarza and Wright, 2010a). Generally, the pervasiveness of the brecciation suggests pedogenesis under semiarid conditions (Platt and Wright, 1992).

5.2. Ostracodal limestones

5.2.1. Observations

Darwinulid (freshwater) ostracodes are the sole invertebrate faunal element in the Ojo Huelos limestones, and are particularly

common in the upper limestone beds in the Carrizo Spring section and throughout the section at Ojo Huelos (Heckert and Lucas, 2002a). At the latter site, the ostracodes are mainly hosted by well-bioturbated micritic wackestones and packstones in which articulated shells filled by calcite spar and pyrolusite dendrites are common (Fig. 9A). Grainstone and packstone beds contain other bioclasts, such as fish bones and scales, and tend to be enriched in organic matter (Fig. 9B). Sedimentary structures are absent within the grainstone beds, although the concentration of fossil debris increases noticeably upward within individual beds. As described below, ostracodes also are common in the porous limestones at the base of the member at Ojo Huelos.

5.2.2. Interpretation

Ostracodes are characteristic of freshwater bodies, although they occur in a wide range of continental environments (De Deckker and Forester, 1988; De Deckker, 2002; Horne et al., 2002). Despite the fact that some ostracodal limestone beds at both Carrizo Spring and Ojo Huelos are extensively rooted, and at the former location also exhibit a brecciated fabric, most of the limestones in this facies lack evidence of subaerial exposure and desiccation. Consequently, deposition in a relatively large water body, e.g., a perennial lake, is envisioned, although water depth was not sufficient to produce dysoxic conditions at the sediment-water interface. Beds in which the concentration of shells increases upward may potentially record shoaling-upward deposition, which implies a sufficiently large fetch to generate wave activity.

5.3. Porous limestone

5.3.1. Observations

Beds of distinctive, brownish-yellow, mottled limestone totaling 0.5 m thick occur at the base of the section at Ojo Huelos. This facies is distinguished by vertically elongated cavities, up to 3 mm wide and 4 cm long, and elongated, vertical gray-brown mottles that display fine dendritic branching (Fig. 10A, B). The rock matrix is dense, dark micritic calcite with irregular hematite stains and irregularly disseminated fine organic matter, and locally contains abundant ostracodes (Fig. 10C). Scanning electron microscopy demonstrates that the micrite is generally quite uniform, comprising crystallites 1 to 2 μm long, and also reveals that a minor authigenic clay fraction is present, likely chlorite (Fig. 10D, E). The matrix is intersected by abundant horizontal veins of calcite spar, 1 to 3 mm wide, locally with a wavy appearance (Fig. 10F). The upper surface of the bed is fine micrite that is less dense than the underlying matrix, and lacks ostracodes or sparry veins.

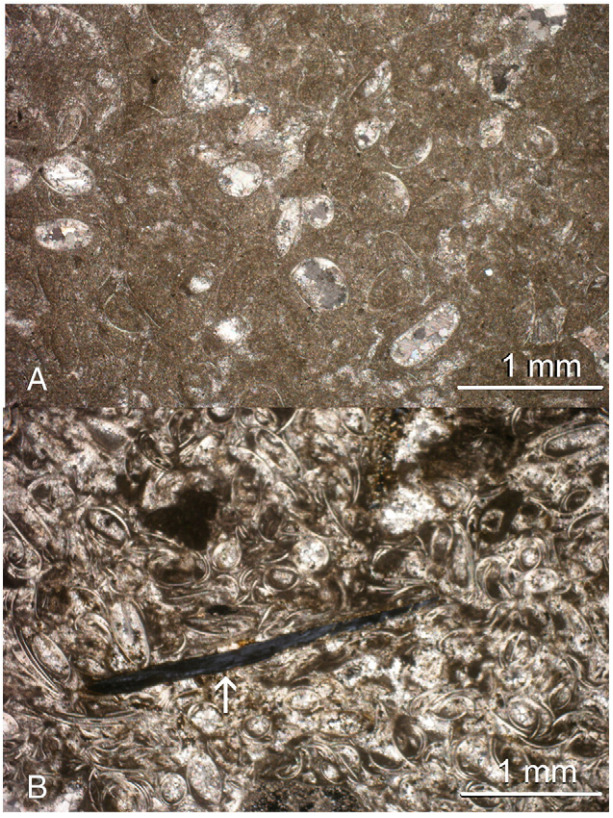

Fig. 9. Ostracodal limestones from Ojo Huelos location. A. Ostracodal wackestone/packstone in which most articulated shells are filled by calcite spar. B. Ostracode grainstone with disseminated organic matter and fish bone (arrow).

5.3.2. Interpretation

The vuggy fabric of this limestone, accentuated in outcrop by weathering, implies biogenic activity, e.g., macrophyte growth, in close contact with the active carbonate sedimentation process, if not actually mediating the process of carbonate precipitation itself. Many of the cavities and the patchy organic matter likely represent the molds and remains of now-decomposed macrophytes, particularly the nearly cylindrical vugs near the top of the unit (see fig. 5C), as seen in many modern and ancient tufas (cf. Rainey and Jones, 2009; Jones and Renaut, 2010). Although the dominant orientation of the voids is vertical, there is a strong component of horizontal fracture-filling calcite spar. This may be a post-depositional feature of desiccation fracturing and calcite re-precipitation. The uniformly fine micrite fabric, however, appears to be the original depositional fabric of the calcite. The microfabric of equant, uniform-size crystallites lacks evidence of cyanobacterial influence, such as tubiform crusts or filaments (cf. Janssen et al., 1999; Merz-Preiß and Riding, 1999). Consequently, we suggest that carbonate precipitation was controlled mainly by abiotic processes, such as outgassing of spring waters.

Carbonates deposited from spring waters are referred to variously as tufa and travertine, with little consistency of usage (see review in Jones and Renaut, 2010). We follow the use of Ford and Pedley (1996) in describing these limestones as tufas, indicating that precipitation took place through dominantly abiotic processes in the presence of macrophytes, and potentially microphytes, and invertebrate fauna (i.e., ostracodes). The pool formed by the spring activity was quite shallow, however, as indicated by the evidence for subaerial exposure, although this pool was sufficiently hospitable to host an ostracode-dominated aquatic fauna. As with other limestone facies in the Ojo Huelos Member, the presence of a micritic veneer with irregular topography on the upper surface of the unit suggests subaerial exposure and incipient karstification of the deposit. The color mottling resulted from iron mobilization during this exposure, and the pattern of this mottling likely was controlled by root penetration of the carbonate mud and changing groundwater level, causing fluctuating Eh conditions.

5.4. Peloidal grainstone/packstone

5.4.1. Observations

This facies forms beds up to 60 cm thick in the three sections at Cañon Agua Buena, but is not well-developed at other locations. Similar to the granular limestone facies of Alonso-Zarza et al. (2011), this facies consists of a framework of well-rounded to subangular grains of micritic carbonate, 0.6 to 3.0 mm in diameter, averaging 2.0 mm (Fig. 11A, B, C). A minor portion of the large framework grains have an irregular shape and consist of hematite-stained clay or mottled micrite, commonly containing silt- to sand-size siliciclastic (e.g., quartz) particles. Some grains have a dark mottled, hematite-stained interior and/or thin, dark hematite rims, and complex internal fabrics, such as brecciation or peloidal clotting (Fig. 11D). Pisoids up to 8 mm comprise

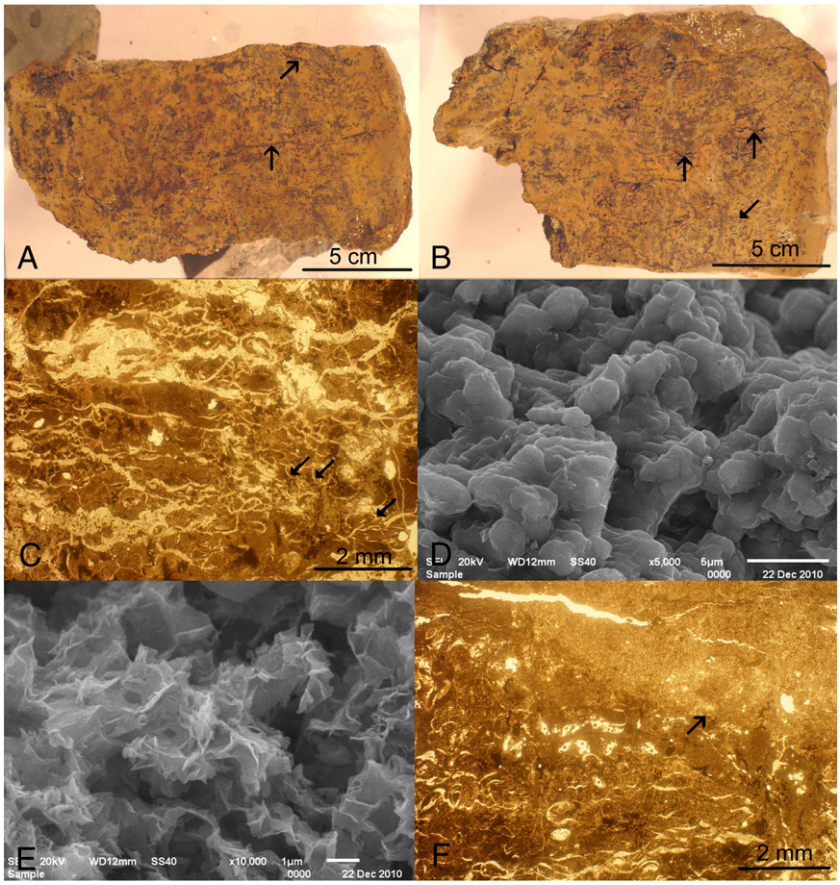

Fig. 10. Features of the basal porous limestone facies at Ojo Huelos. A, B. Hand samples of the basal limestone unit, top to the right. Both slabs exhibit characteristic mottling and vuggy porosity. In A, vertically elongated, branching to dendritic mottles (arrows) are prominent. In B, vugs vary from millimeter-scale and irregular shape (lowest arrow) to vertically elongate, centimeter scale (upper arrows). A thin veneer of slightly lighter-color limestone is visible forming the top of the sample in B. C. The limestone contains abundant ostracodes (arrows) and hosts a network of spar-filled veins and dispersed organic matter. D. SEM micrograph of the micrite in the basal limestone illustrates the relatively uniform crystallite size. E. A minor clay fraction consists primarily of authigenic chlorite (SEM micrograph). F. Section from the top of the unit demonstrates the contrast in fabric between the dense, fossiliferous, organic-rich micrite that comprises most of the basal unit and the lighter micritic veneer at the top (arrow).

a minor proportion of the grain framework. The matrix between the grains varies from mostly detrital (chloritic) clay, with minor silt- to sand-size grains of siliciclastic particles, to a combination of sand-size grains of quartz, smaller micritic calcite clasts and bioclasts (fragments of ostracodes, and phosphatic fish scales and bones) in a sparry calcite cement (Fig. 11E). The peloids in the grainstones locally host a fringing cement of bladed calcite (Fig. 11F). Peloidal packstones with clayey matrix show complex grain contacts, ranging from concavo-convex to sutured, whereas sparry-cemented grainstones display dominantly point contacts.

5.4.2. Interpretation

Alonso-Zarza and Wright (2010a) and Alonso-Zarza et al. (2011) classify peloidal packstones and grainstones as palustrine limestones because the origin of the carbonate grains ultimately is the repeated desiccation reworking of the previously deposited carbonate sediments, a process described by Wright (1990) as grainification. We note, however, that although pedogenic processes can indeed produce the well-rounded shape of the major framework grains observed here, the presence of the mixed framework, including siliciclastic grains and irregularly-shaped, hematite-stained argillaceous clasts, indicates further erosion and re-deposition of the micritic carbonate as part of the bedload of a traction current. Additionally, we note the lack of evidence for root penetration in these beds, indicating that deposition took place separately from the process of grainification.

A lacustrine origin for at least some, if not all, of the carbonate grains is inferred from the presence of bioclasts with a lacustrine affinity (i.e., fish and ostracode debris), which suggests that the peloidal limestone clasts were derived from intense brecciation of the palustrine carbonate. Transport and rounding of the clasts required an energetic traction current, although the direction (or directions) of transport are not indicated. The association of the peloidal facies at Cañon Agua Buena with the pisolitic and cross-bedded sandstone facies described below suggests that Ojo Huelos deposition at this particular location was dominated by stream processes.

5.5. Pisolitic rudstone

5.5.1. Observations

Beds consisting of pisoids with mudstone and micritic calcite clasts, the latter as subordinate framework components, occur most prominently in the sections at Cañon Agua Buena (Fig. 12A), where they are up to 1.6 m thick, but occur also less prominently at Carrizo Spring, San Pedro Arroyo and Weber, at which locations the pisoids appear less distinct than at Cañon Agua Buena, and lack organized bedding. At Cañon Agua Buena, pisolitic rudstone beds are massive to crudely horizontally stratified, and many of the beds exhibit upward fining of the pisoids. Notably, the individual beds are not correlatable between outcrops spaced several hundred meters apart.

The pisoids are up to 3 cm in diameter and consist of crudely concentric bands of microspar to sparry calcite bands and hematite-stained, calcareous silty mudstone. The matrix of the rudstone consists of a mix of

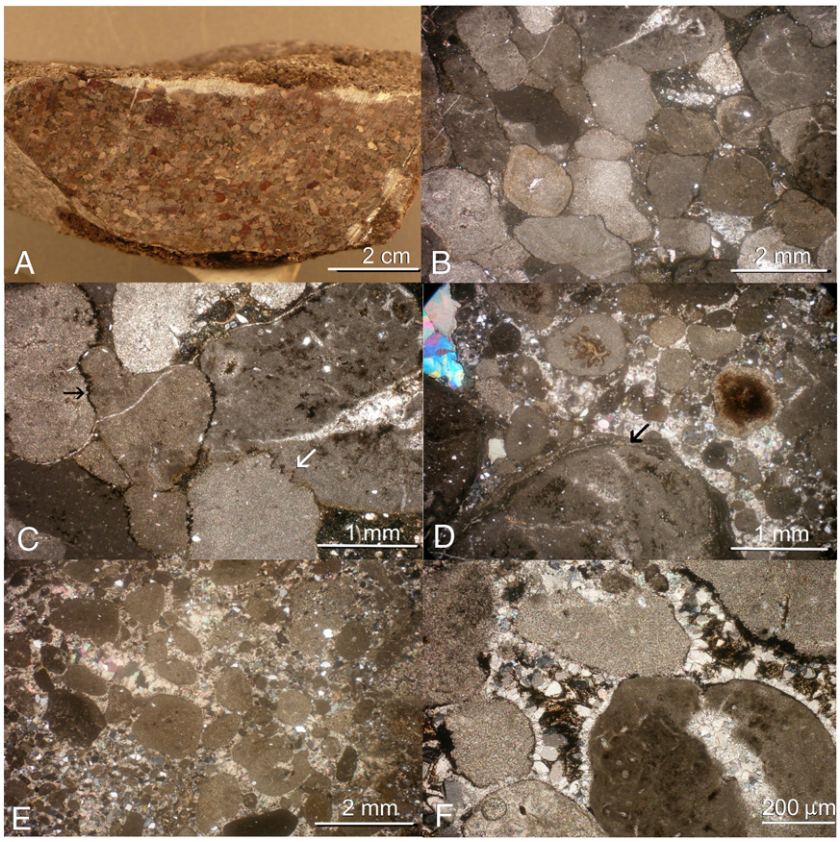

Fig. 11. Features of peloidal grainstone lithofacies. All samples from Cañon Agua Buena. A. Hand specimen illustrates the tightly packed grain fabric, comprising mainly granule-size peloids with some mudstone clasts. B. In thin section, it is evident that the grains are predominantly rounded particles of micrite. C. Peloidal grainstone with tight packing in which grain contacts are commonly sutured (arrows). D. Some larger peloids have complex, multiple-generation rims (arrow). The cores of some other grains display concentrations of hematite. E. The matrix of this grainstone contains abundant siliciclastic grains, mainly quartz. F. Peloids in this grainstone are surrounded by a fringe of bladed calcite cement that extends outward from the grain into the clayey matrix.

siliciclastic sand grains, mostly quartz, but also chert, and smaller calcareous mudstone clasts that are hematite stained, in places with interpenetrating grain contacts, all in a sparry calcite matrix. Larger pisoids have a complex structure of alternating layers of sparry calcite, radiating (palisadic) calcite and hematite-stained argillaceous calcite laminae, all surrounding one or more central nuclei of micritic to sparry, radiating calcite bodies (Fig. 12B–G), atypically with broken cortices (Fig. 12H).

5.5.2. Interpretation

The organization of the pisolitic rudstone into tabular, massive to stratified beds, locally upward-fining, demonstrates deposition of the pisoids by traction currents. As for the peloidal limestones described above, the pisolite beds lack evidence of root penetration. Additionally, the rudstone beds at Cañon Agua Buena are overlain by and interbedded with planar-tabular, cross-bedded sandstone. Consequently, we interpret the pisolitic rudstone beds as the gravel bars of energetic, high-bedload, low-sinuosity streams (Miall, 1977; Miall,1978; Miall, 1996).

This does not explain the origin of the pisoids, however. Coated grains (pisoids, oncoids) are known to form in a wide variety of terrestrial settings, including lacustrine (Freytet and Plaziat, 1982; Davaud and Girardclos, 2001; Shapiro et al., 2009), stream travertines (Guido and Campbell, 2011) and mature calcrete paleosols. In regard to the latter, the pisoidal coatings are considered a beta fabric, i.e., a calcrete feature with a biogenic origin (Wright, 2007; Zhou and Chafetz, 2009). Individual laminations are sometimes low-relief, but often crenulitic (Fig. 13A, B), locally-domed, resembling microstromatolites (Shapiro et al., 2009). This is consistent with a bacterial role in the formation of the layering, although this biogenic activity could have occurred in any of the environments listed above.

The association of the pisolitic facies at Cañon Agua Buena with the peloidal gainstone/packstone facies, and the presence of some pisoids in the latter, suggest that the origin of both facies may be related. We interpret the pisoids as the product of intense pedogenic reworking of the palustrine carbonate, as with the peloidal facies, that was subjected to subsequent erosion and fluvial re-deposition. This mode of deposition of the pisoids is confirmed by the interbedding of the rudstone with the litharenite sandstone facies (see below). The nuclei of the pisoids are fragments of the original lacustrine/palustrine carbonate mud, recrystallized in many cases, that were dislodged and rotated repeatedly by pedogenesis, allowing microbial activity to mediate precipitation of the cortices. The pisolitic rudstone in the Weber section, which has a distinctly less-developed fabric than the outcrops at Cañon Agua Buena (Fig. 13C), may exemplify the progressive formation of the pisoids in the palustrine carbonate. Similar pisoids within the channel conglomerates of the Upper Siwalik Formation (Pleistocene) of northern India were described by Tandon and Narayan (1981) as reworked calcrete.

5.6. Nodular limestone

5.6.1. Observations

Mudstones in several sections (Cañon Agua Buena, Carrizo Spring) host horizons of nodular limestone that weather to form prominent benches on slopes. Typically, this facies occurs near the top of the Ojo Huelos Member, i.e., above most of the carbonate facies described above. The limestones range from calcareous masses hosted by blue-gray mudstone, to slightly argillaceous, nodular limestone beds. Both types of nodular limestone beds typically display extensive root traces and weather to form prominent benches on slopes. The

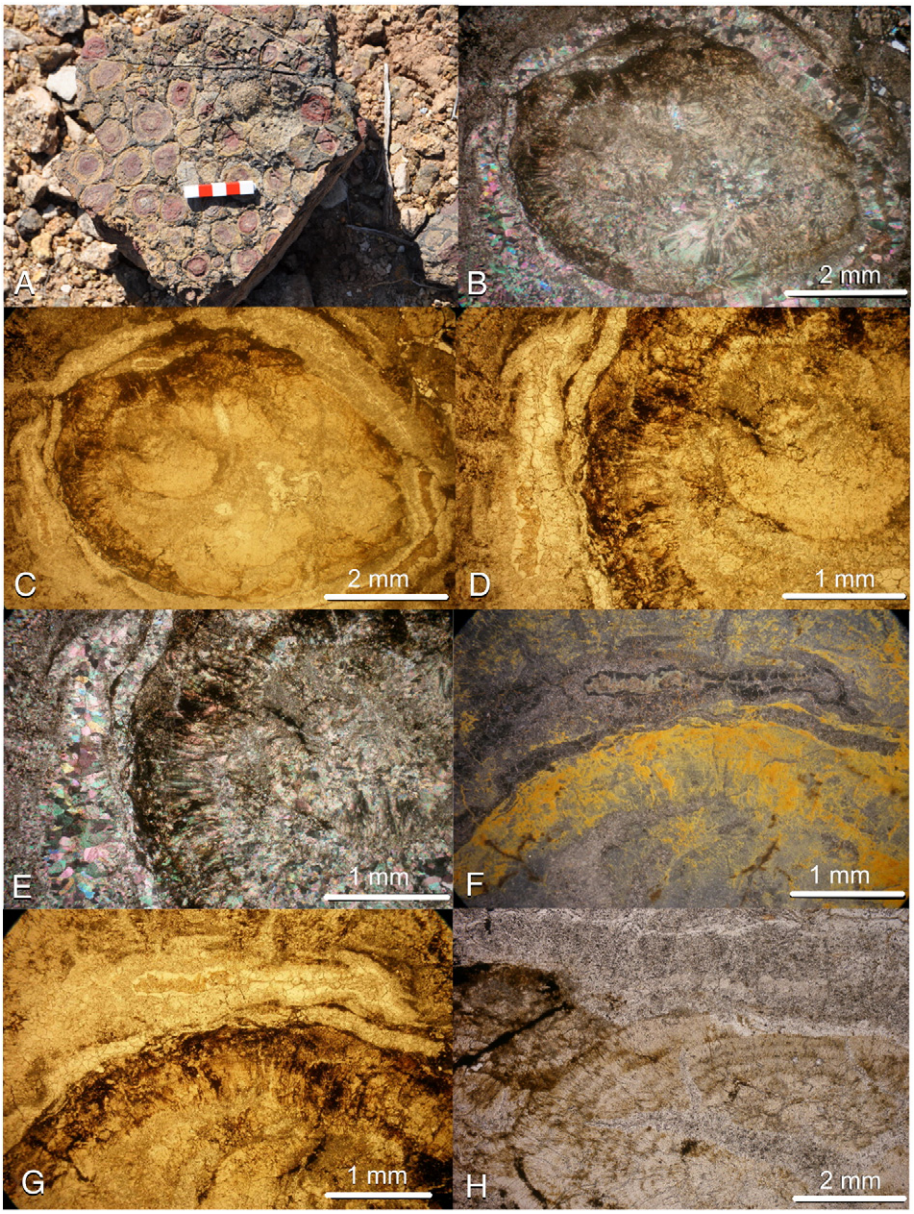

Fig. 12. Features of pisolitic rudstone lithofacies. All samples from Cañon Agua Buena. A. Field photograph of typical pisolitic rudstone illustrating concentric layering of most of the pisoids, many of which have hematite-enriched cores. B (nicols crossed), C (nicols uncrossed). Interiors of individual pisoids often have complex structure, as shown here with three separate core masses of calcite with radiating fabric. D (nicols uncrossed), E (nicols crossed). Detail of B, C illustrating variations in thickness of cortices, ranging from palisadic (inner cortex) to equant spar (outer cortices). F (reflected light image), G (nicols uncrossed). Hematite (reddish-brown in F) is distributed unevenly within thick inner cortex, with concentration increasing from inner to outer laminae. G. A small number of pisoids have broken cortices.

mudstone-hosted calcareous nodule horizons are 0.3 to 0.8 m thick. The micritic nodules vary in shape from subspherical to irregularly globular (botryoidal), 2 to 7 cm in diameter, and typically have diffuse boundaries. The nodular limestone beds, up to 0.5 m thick, are typically pebbly and are composed of amalgamated calcite nodules up to 5 cm (Fig. 14A). Pebbly nodular limestone displays floating grains, with notable corrosion of quartz grain boundaries, and grain coronas of bladed calcite (Fig. 14B).

5.6.2. Interpretation

The association of roots with the nodular limestones suggests a pedogenic origin for the carbonate. Additionally, features typical of alpha-type calcrete fabrics, such as the grain coronas and corroded floating grains demonstrate that these beds represent the accumulation of carbonate in the B horizon of paleosols (Alonso-Zarza and Wright, 2010b). Consequently, we interpret the carbonate beds of this facies as calcretes formed within soils developed on alluvial muds. These mudstone-hosted calcareous nodule horizons represent simple Stages II to III calcrete profiles (Gile et al., 1966; Esteban and Klappa, 1983; Machette, 1985). Stage II profiles comprise isolated nodules in discrete horizons with gradational bases and tops, whereas the more mature Stage III profiles consist of coalesced horizons in which the nodules are generally vertically stacked.

5.7. Brecciated calcareous mudstone

5.7.1. Observations

Beds up to 60 cm thick of calcareous mudstone with an obvious brecciated fabric that is evident both in the field and in hand specimen occur in the sections at San Pedro Arroyo and Weber. The mudstone is dark reddish brown and forms a network of equant to irregular blocks that range in size from 200 μm to a maximum of

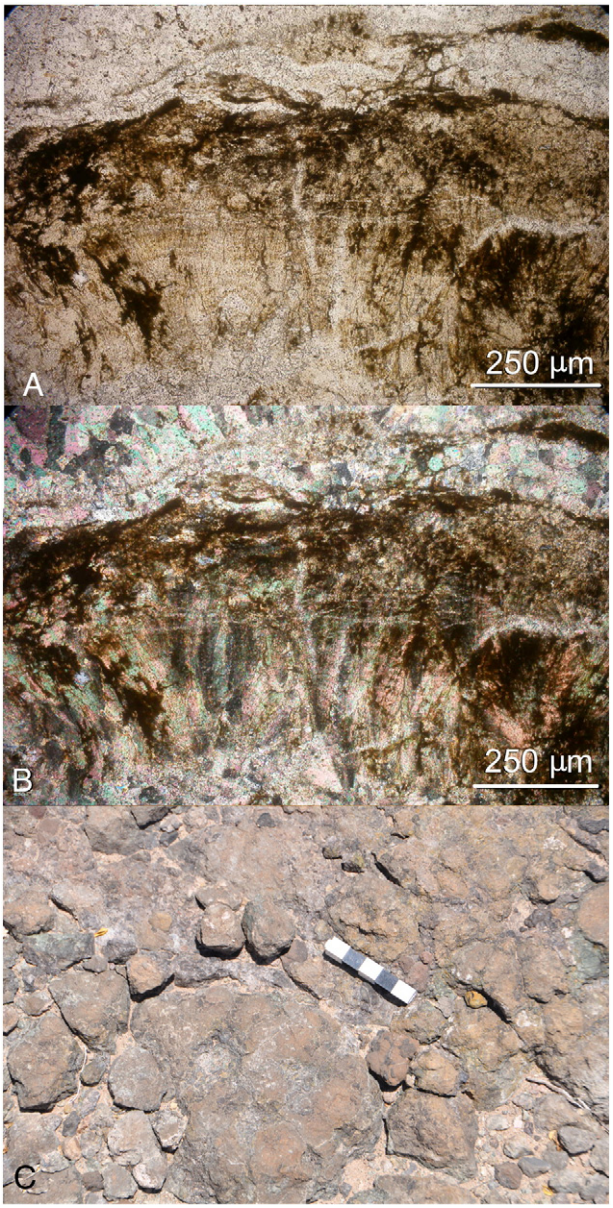

Fig. 13. Features pertaining to the origin of the pisoids. A (nicols uncrossed), B (nicols crossed). Interior cortex of this pisoid consists of palisadic calcite coated by irregular, locally thin, crenulitic to domed hematite coatings. Sample from Cañon Agua Buena. C. Upper limestone bed at Weber displays crude pisoids with diffuse boundaries. Scale bar = 5 cm.

2 cm, typically 0.5 cm (Fig. 15A). In the section at Weber, the brecciated mudstone facies is in depositional contact with brecciated limestone (Fig. 15B). Root traces that are drab greenish gray, contrasting with the mudstone, are locally common, particularly near the tops of beds, where they penetrate 10 cm, tapering and branching downward (Fig. 15C). The mudstone blocks commonly form a near-interlocking, or jig-saw fabric, with adjacent blocks separated by 1- to 2 mm-wide veins that are white to drab gray (Fig. 15D, E). The veins typically consist of calcite spar with 100 μm crystals. Locally, the veins are vertical and branching, superficially resembling root traces, but more commonly they form a reticulated network of perpendicular, intersecting vertical and horizontal veins. The mudstone clasts commonly have a complex internal structure comprising multiple domains, each characterized by a variable component of silt-size siliciclastic grains, discrete grains of micritic carbonate, and organic content in clayey matrix that is stained unevenly by hematite. Locally, grains of hematite-stained mudstone are surrounded by a fringe of micritic calcite, 100 μm wide (Fig. 15F).

5.7.2. Interpretation

Significantly, the mudstone blocks of this facies typically exhibit the jig-saw facies of nearly interlocking fragments and generally lack evidence of rounding, suggesting that the grains have not been transported; i.e., this texture formed *in situ*. Although root traces are locally common in the facies, they do not appear to be the dominant structure forming the separations between the blocks. Rather, discrete calcite-filled veins form the divisions.

Alonso-Zarza et al. (2011) labeled a very similar mudstone texture, also associated with palustrine carbonate facies, as "desiccated mudstone," formed, as the name suggests, by the desiccative brecciation of muddy sediments. Thus, the brecciated mudstone facies is a pedogenically-modified sedimentary deposit; in essence it constitutes a blocky ped fabric, formed by repeated wetting and drying, infused by an early diagenetic carbonate cement. Although not a calcrete by definition, the carbonate cement in the brecciated mudstone displays some features associated with alpha-type calcretes, such as grain coronas and sparry vein fills (Wright, 2007; Zhou and Chafetz, 2009).

5.8. Litharenite sandstone

5.8.1. Observations

Beds of pale yellow to tan sandstone are conspicuous for their presence only at the three Cañon Agua Buena sections. The sandstone is fine-grained to very-fine grained and micaceous, well-sorted litharenite (40% metamorphic rock fragments, 10% feldspar). The thickest sandstone section overlies the pisolite beds and forms tabular sets up to 0.6 m thick, but higher in the section the sandstone occurs as sets of trough cross-beds 0.2 to 0.3 m thick, and also as lenticular beds encased in slope-forming mudstone near the top of the section. Climbing ripples occur in a single bed near the base of the section at only one of the Cañon Agua Buena sections.

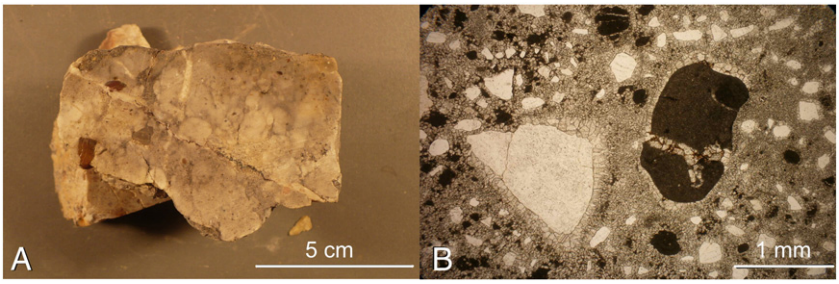

Fig. 14. Features of nodular limestone lithofacies. Samples from Carrizo Spring. A. Hand sample shows centimeter-scale nodules of micritic calcite with sharp to diffuse boundaries in calcareous matrix containing substantial siliciclastic sand and pebble content. Top to the right. B. Matrix of nodular limestone displays prominent bladed-calcite coronas surrounding large quartz (light) and mudstone (left) grains set in microspar.

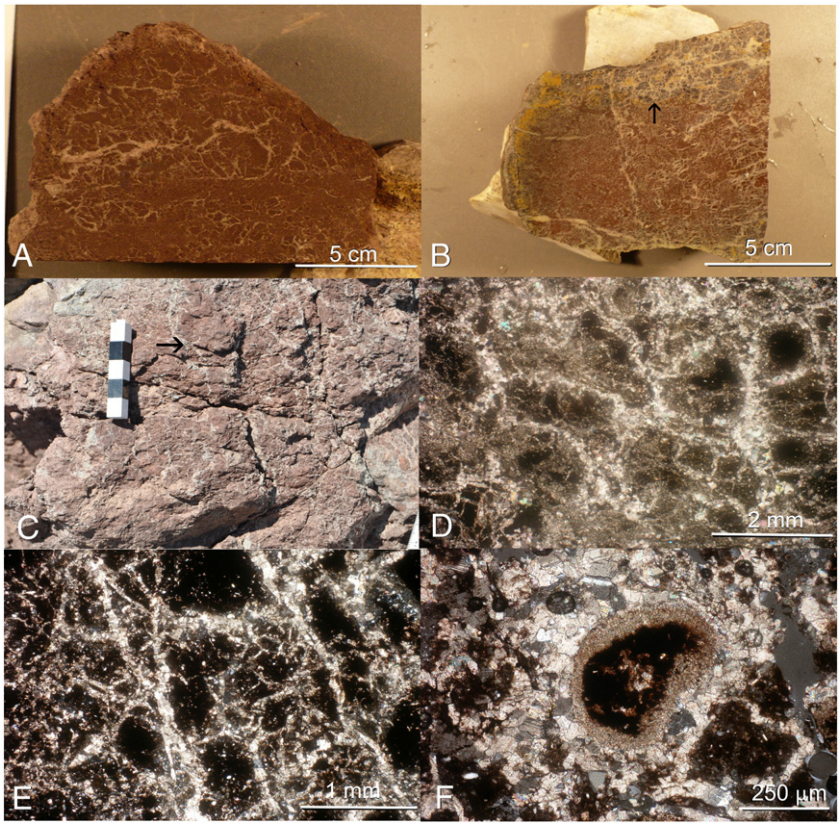

Fig. 15. Features of the brecciated mudstone lithofacies. A. Hand sample from San Pedro Arroyo displays typical jig-saw fabric of interlocking mudstone blocks separated by calcite veins. B. Sample from the section at Weber contains contact between brecciated mudstone and brecciated limestone lithofacies (arrow). C. Field photo from San Pedro Arroyo shows drab, branching root traces (arrow) in addition to reticulated pattern of veins intersecting the mudstone. D, E. Mudstone blocks, 1 mm to 3 mm, with sharp boundaries separated by thin veins of sparry calcite, with some blocks complexly fragmented. F. Some mudstone grains have a fine micritic halo.

5.8.2. Interpretation

Although limited outcrop exposure does not permit interpretation of the fluvial architecture, the sandstone beds display various sedimentary structures that record the migration of bedforms in streams, i.e., bars, dunes and ripples, under varying conditions of sediment load and flow regime. The association in section A at Cañon Agua Buena of the sandstones with both pisolitic rudstone, which underlies the sandstone, and mudstone, which overlies it, indicates initially energetic, high-bedload transport, but with gradually decreasing stream competence (Miall, 1996). The transition from planar cross-beds to trough cross-beds is a change in bedform, from bars, either mid-channel or side-attached to dunes, likely recording a decrease in the sediment load of the stream. Lenticular sandstones encased in mudstone demonstrate a transition in stream transport from bedload-dominated to suspended-load dominated, possibly accompanied by increasing channel sinuosity (Miall, 1977, 1996; Fielding et al., 2011).

6. Facies model

Analysis and interpretation of the facies described above, combined with their vertical and lateral relationships, allows reconstruction of the Late Triassic (late Carnian or early Norian) landscape on which the Ojo Huelos sediments were deposited (Fig. 16). Following deposition of the coarse-grained streams of the Shinarump Formation, which infilled paleovalleys incised into the underlying Moenkopi Formation strata (Stewart et al., 1972; Blakey and Gubitosa, 1983; Demko et al., 1998), fine-grained siliciclastic sediments of the San Pedro Arroyo Formation were deposited across a low-gradient, muddy alluvial plain. The transition from the high-bedload Shinarump system to the suspended-load dominated San Pedro Arroyo system, which demonstrates completed burial of the pre-Chinle paleotopography (Tanner and Lucas, 2006), is easily observed in the section at San Pedro Arroyo where the Shinarump gravel conglomerates are overlain by interbedded mudstones, cross-bedded sandstones and intraformational conglomerates, and overlain in turn by slope-forming mudstones.

Ponds and lakes formed on the alluvial plain that were at least in part spring fed, as demonstrated by the interpreted tufa deposit at the base of the section at the Ojo Huelos location. These lakes and ponds were the sites of partly or potentially largely abiogenic carbonate precipitation and accumulation, in part due to a lack of siliciclastic input (Tucker and Wright, 1990; Platt and Wright, 1991; Carroll and Bohacs, 1999). Additionally, they hosted a diverse vertebrate fauna, with an invertebrate fauna that was dominated by ostracodes. The water bodies were of varying size, although the potential size is limited, as suggested by the lack of deeper water facies. However, sufficient fetch to generate wave activity and shoreline facies is suggested by the ostracodal grainstone in the Ojo Huelos section, analogous to the interpretation of coarse-grained carbonate facies in the Triassic Mercia Mudstone Group of South Wales (Talbot et al., 1994; see also Gierlowski-Kordesch, 2010).

Episodic changes in the regional water table, or hydrologic base level, caused fluctuation in the size of the water bodies; base-level fall caused shoreline withdrawal and subjected the carbonate sediments to pedogenesis, i.e., repeated episodes of wetting/drying and root penetration. Variations in the degree of brecciation reflect differences in the intensity of pedogenic reworking. These variations were controlled ultimately by water depth; marginal (palustrine) environments, such as wetlands and low-energy shorelines were exposed more completely and for longer periods than were perennially submerged environments. Ancient carbonates displaying similar features that have been interpreted as carbonate pond deposits include the

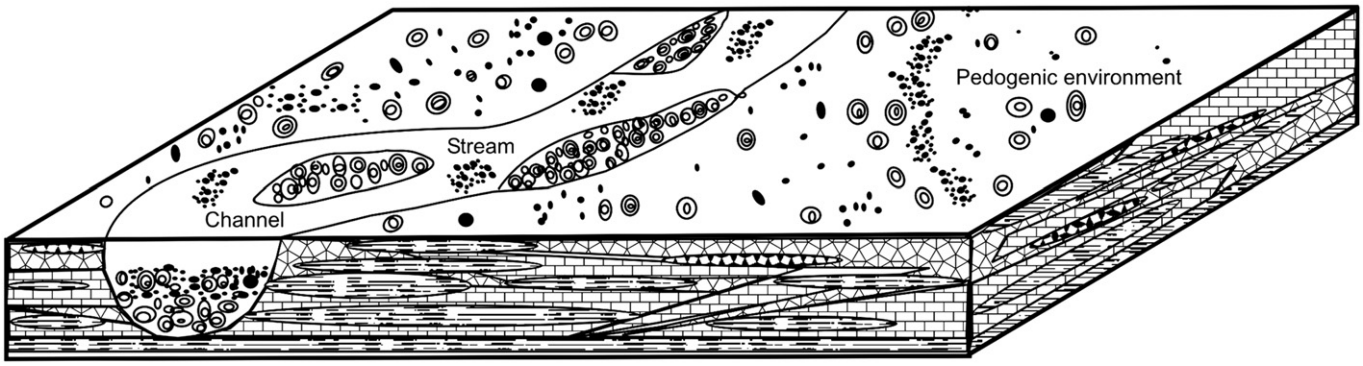

Fig. 16. Idealized paleogeographic reconstruction of the Ojo Huelos depositional landscape illustrating degradational processes. Deposition of carbonate and siliciclastic mudstone occurred initially in lakes, ponds and marshes, as well as on muddy alluvial plains, above the mudstones of the Araya Well Member. During lowstand intervals, pedogenic reworking of the sediments produced peloids (smaller grains) and pisoids (larger grains). Subsequent erosion of the landscape mobilized these grains, which then formed the bedload fill of a channel incised into the landscape at Cañon Agua Buena. All lithologic symbols as in Fig. 3.

Upper Triassic Mercia Mudstone Group of England (Talbot et al., 1994), the Miocene Intermediate Unit of the Madrid Basin (Sanz et al., 1995) and the Upper Triassic Owl Rock Formation of the Chinle Group on the Colorado Plateau (Tanner, 2000). Alonso-Zarza et al. (2006) described similar features in the modern Las Tablas de Daimiel wetlands in Spain and suggested that these are an appropriate modern analog for the interpreted palustrine carbonates seen in the ancient record.

Sediments subjected to the most intense pedogenesis may have experienced significant replacement of the carbonate by chert, as at Carrizo Spring (Bustillo, 2010). These differences in the degree of exposure are manifested in the significant lateral variations in the degree of pedogenic alteration of the micritic limestone facies, visible at the outcrop scale in the sections at San Pedro Arroyo and Carrizo Spring. The limestones in the Ojo Huelos section, which are the most fossiliferous among any of the sections studied, exhibit the least pedogenic alteration, and therefore most likely represent deposition in a deeper (i.e., perennial) lacustrine setting. Mudstones interbedded with the limestones were deposited during episodic influxes of fine-grained siliciclastic sediments, but these also were subjected to wetting/drying cycles, resulting in the brecciated mudstone facies interbedded with the limestones at San Pedro Arroyo and Weber.

Episodes of more severe and prolonged base-level (water table) fall resulted in the degradation of the landscape as the pedogenically-brecciated lacustrine and palustrine sediments were remobilized by erosion and transported, potentially by sheetflow, into streams, resulting in the deposition of the peloidal limestones as gravelly sheets and bars (Alonso-Zarza et al., 1992, 2011). Formation of incipient pisoids is seen in limestone beds with crude pisoids near the top of the Ojo Huelos Member sections at Carrizo Spring, Weber and San Pedro Arroyo, but pisolitic rudstone- and sandstone-filled channels dominate the Cañon Agua Buena section, which largely lacks the micritic/brecciated limestone facies. Notably, thickly bedded pisolitic rudstones like those at Cañon Agua Buena do not occur elsewhere, even at the Weber section, only ~4 km distant. Consequently, we interpret most of the Cañon Agua Buena section as recording deposition of a stream that scoured into the Ojo Huelos landscape and filled initially with pisoids derived from reworked paleosols (Tandon and Narayan, 1981) and later with extrabasinal sediment. The incised valley had erosional relief of approximately 16 m, based on the thickness of pisoid gravel and sandstone bar and dune deposits that filled the channel. Sedimentation and landscape aggradation resumed with the deposition of alluvial mudstone and minor lacustrine limestones, burying the erosional topography, but with brief interruptions caused by base-level fall, as recorded by calcretes and peloidal limestones, as at Cañon Agua Buena and Carrizo Spring.

7. Discussion

7.1. Base-level control

Deposition of the San Pedro Arroyo Formation can be viewed in part as a response to regional changes in hydrologic base-level. The landscape aggraded as base level, controlled by the water table, rose, causing deposition of the alluvial muds and sands of the Araya Well Member. The aggradational sequence was capped by lacustrine–palustrine limestones that accumulated as the siliciclastic sediment supply waned. Base-level low-stand resulted in extensive pedogenesis of the limestone and laterally equivalent alluvial facies. Tanner (2000), for example, modeled the interbedded alluvial clastic/carbonate succession of the Upper Triassic Owl Rock Formation as aggrading sequences of alluvial sediments deposited during base-level rise, capped by highstand carbonates that were deposited in small perennial and ephemeral carbonate lakes and ponds. Ancient successions of interbedded alluvial clastics and carbonates also have been interpreted as the result of autocyclicity, in which carbonate deposition is attributed to reduced siliciclastic input to areas that are isolated from the primary site of sedimentation, such as interchannel lows on a floodplain (Calvo et al., 1989; Sanz et al., 1995); this may explain the lack of lateral continuity of individual limestone beds.

Alluvial systems have predictable responses to base-level changes; aggradation during base-level rise is common as streams attempt to maintain constant gradient (Schumm, 1993). But, potential allocyclic controls on base level are varied, including eustasy, tectonics, and climatic control of basin hydrology, and not always easily discerned from the sedimentary record. Eustatic control of the aggradational sequences in the San Pedro Arroyo Formation is highly improbable given the likely 700 km or more separation between the study area and the shoreline of the back-arc seaway (Ethridge et al., 1988; Schumm, 1993; Marzolf, 1994; Rogers, 1994). Variations in rates of uplift and subsidence have been cited as controls on base-level variations during deposition of other parts of the Chinle Group, such as the Petrified Forest Formation (Kraus and Middleton, 1987), as evidenced by volcanic ash layers, indicative of arc-magmatic activity and potential source-area uplift (Stewart et al., 1986), but there is no evidence for such activity in the San Pedro Arroyo Formation.

Sequences of alternating alluvial mudstone and lacustrine-palustrine carbonates similar to the San Pedro Arroyo Formation have been attributed to climatically driven base-level fluctuations (Talbot et al., 1994; Tanner, 2000), with siliciclastic deposition dominating during lowstand and carbonate deposition occurring during highstands. The Ojo Huelos depositional sequence appears to have operated basinwide, and so may have resulted principally from changing base

level, driven by climate-controlled basin hydrology. Deposition of the Araya Well Member coincided with a period of high humidity, with heightened fluvial discharge and sediment transport to the floodbasin, resulting in positive sediment accumulation and basinwide aggradation. Carbonates capped the aggradational sequences as small perennial and ephemeral lakes and ponds filled low areas on the floodplain created by stream migration and avulsion. Extended periods of nondeposition and degradation occurred on the floodplain during base-level fall and lowstand as pedogenesis modified highstand deposits. Climatic fluctuations, therefore, may have controlled deposition of the aggradational cycles, as has been interpreted for the younger Owl Rock Formation (Tanner, 2000).

Orbital control of climate during the Late Triassic is well documented from the rift basins of the Newark Supergroup (cf. Olsen, 1986; Olsen and Kent, 1996), where base-level changes manifested as transgressions and regressions of lakes occupying the rift basins at apparent periodicities of 23 kyr, 100 kyr and 400 kyr. Similar orbital control of the hydrologic base level in deposition of Chinle Group strata has been suggested previously, but as Tanner (2000) pointed out, the temporal control of the stratigraphy is lacking to demonstrate periodicity. Hence, orbital control of the base-level fluctuations evident in the San Pedro Arroyo Formation is necessarily speculative.

7.2. Paleoclimate

The deposition of carbonate sediments in lacustrine environments is often associated with semi-arid settings on the assumption that the aqueous carbonate concentration in humid-setting lakes is likely to be too dilute to allow appreciable precipitation; additionally, the accompanying high siliciclastic influx from surface run-off will dilute carbonate sediments (Dean, 1981; Cecil, 1990; Platt and Wright, 1991; Sanz et al., 1995; De Wet et al., 1998; Gierlowski-Kordesch, 1998). Yet, evidence of semi-aridity, in the form of evaporites or stromatolites interbedded with the lacustrine carbonates (Platt and Wright, 1991), is lacking in the Ojo Huelos section. As noted by Tanner (2010), however, the presence of lacustrine carbonates is by itself not an indicator of climate, and in fact, the majority of modern carbonate lakes occur in temperate, humid settings. Bohacs et al. (2000) pointed out that lakes may display tremendous variations in size, chemistry and sedimentation style, regardless of climate, as a consequence of very local controls.

Conversely, the formation of the characteristic textures of palustrine carbonates is very sensitive to changes in hydrology, and consequently, to variations in precipitation or groundwater levels. There exists a variety of features that are indicative of water availability during the formation and subaerial exposure of palustrine sediments. For example, organic-rich lithologies have a higher preservation potential in semi-humid than in semi-arid climates, while greater aridity will cause more intense desiccation, with consequent development of brecciated and peloidal fabrics, microkarst surfaces and, with greater aridity, the formation of evaporites that may be altered subsequently to chert (Alonso-Zarza et al., 1992; Platt and Wright, 1992; Alonso-Zarza, 2003; Bustillo, 2010).

Previous studies have interpreted gradual drying of the climate of the Colorado Plateau region during the Late Triassic, as suggested from lithofacies and pedofacies transitions in Chinle Group strata (Dubiel, 1994; Tanner, 2000; Tanner and Lucas, 2006). A humid but strongly seasonal climate during basal Chinle deposition is indicated by gleyed kaolinitic and illuviated paleosols in strata of the Shinarump and Zuni Mountains formations (Tanner and Lucas, 2006, 2007). The age of these strata is in dispute, however. As described in Section 2, the Adamanian LVF is interpreted variously as late Carnian or early-middle Norian (Lucas et al., 2012). By either interpretation, however, the interval of Ojo Huelos deposition postdates the well-documented Carnian pluvial event, dated by most workers as early Carnian to middle Carnian (latest Julian to early Tuvalian; Simms and Ruffell, 1990; Simms et al., 1994; Kozur and Bachmann, 2010; Roghi et al., 2010). The strata of the Cameron, Monitor Butte and Bluewater Creek formations, all of which occupy the same stratigraphic position as the San Pedro Arroyo Formation, and the overlying Blue Mesa Member of the Petrified Forest Formation, contain paleosols that are primarily vertic Alfisols, locally calcic (stages II to III calcretes) to gleyed (Tanner, 2003; Tanner and Lucas, 2006). These pedogenic features suggest a strongly seasonal, but possibly subhumid climate (Tanner, 2003; Tanner and Lucas, 2006). However, the palustrine textures described in this paper for the Ojo Huelos Member of the San Pedro Arroyo Formation are more indicative of episodes of semi-arid climate for this same time interval. Thus, the intervals of landscape degradation during Ojo Huelos deposition appear to mark a transition from more humid, but strongly seasonal climate during basal Chinle deposition to alternating subhumid to semi-arid conditions that are more characteristic of the upper Chinle Group. This climate transition is consistent with paleomagnetic evidence for a northward translation of the North American continent during the Late Triassic of over 15° (Kent and Tauxe, 2005), carrying the central New Mexico region from a near equatorial location to a drier, subtropical latitude.

7.3. Regional context

On the Colorado Plateau (northwest of the study area), the strata that occupy the position equivalent to the San Pedro Arroyo Formation are the Cameron, Bluewater Creek, and Monitor Butte formations (Lucas, 1991; Lucas, 1993; Lucas et al., 1997; Spielmann and Lucas, 2009). These strata, of late Carnian age, consist mainly of gray bentonitic to variegated mudstones, dark shales, and laminated to cross-bedded, fine-grained sandstones (Heckert and Lucas, 2002a). Although thin micritic limestone occurs locally near the base of the Bluewater Creek Formation (Heckert and Lucas, 2002b), no distinctively lacustrine carbonate beds have been described previously from the stratigraphic interval comprising the lower Chinle Group. Therefore, the occurrence of the thick (meter-scale), bedded limestones in the Ojo Huelos Member is an anomaly within the lower Chinle Group.

Understanding basin hydrology is important in differentiating tectonic and climatic controls on deposition of lacustrine and palustrine carbonates, as demonstrated by recent work on the Upper Jurassic Morrison Formation (Dunagan and Turner, 2004; Jennings et al., 2011). The presence of the Ojo Huelos carbonates in central New Mexico may be primarily a function of regional hydrology. The study area is located more proximal to the inferred position of the sediment-source area in the Mogollon highlands, approximately 200 km to the south and southwest, than other described lower Chinle outcrops (Marzolf, 1994). These highlands would also have been the recharge area for the regional hydrology, fed by southeast-blowing trade winds (Peterson, 1988). Hence, the Ojo Huelos carbonates were located in an area of higher ground-water availability and spring discharge than locations more distal to the Mogollon Highlands.

8. Conclusions

The Ojo Huelos Member of the San Pedro Arroyo Formation comprises a spectrum of carbonate lithofacies, including micritic to brecciated limestones, peloidal grainstones and packstones, and pisolitic and nodular limestones, that record the formation on a low-gradient alluvial plain of shallow water bodies and wetlands of various sizes in which carbonate sedimentation took place. These bodies were likely in-part spring-fed, as indicated by the interpreted tufa limestone. The lakes and ponds were subject to episodes of shrinking, during which the lacustrine and palustrine carbonate sediments were subjected to pedogenic processes, such as desiccation and rooting. Falling base-level,

likely driven by episodic aridification of the climate and the consequent change in regional hydrology, caused intervals of degradation of the landscape, with erosional reworking of the pedogenically-modified carbonates, and significant fluvial incision, with a substantial portion of the channel fill derived from reworked calcrete.

Recognition of the palustrine fabrics in the limestones and the pedogenic origin of the peloidal and pisolitic lithofacies indicate that a transition from humid to alternating subhumid-semiarid climate was responsible for the hydrologic changes. Furthermore, this interpretation demonstrates that the long-recognized aridification of this region during the Late Triassic commenced at least by the early part of the Norian.

Acknowledgments

Field work for this study was supported in part by the Provost's Discretionary Fund of Le Moyne College. The manuscript benefitted from the constructive comments of Elizabeth Gierlowski-Kordesch and two anonymous reviewers, as well as the editorial assistance of Brian Jones.

References

Alonso-Zarza, A.M., 2003. Palaeoenvironmental significance of palustrine carbonates and calcretes in the geological record. Earth-Science Reviews 60, 261–298.

Alonso-Zarza, A.M., Wright, V.P., 2010a. Palustrine carbonates. In: Alonso-Zarza, A.M., Tanner, L.H. (Eds.), Carbonates in Continental Environments: Processes, Facies and Applications. Developments in Sedimentology, 61. Elsevier, Amsterdam, pp. 103–131.

Alonso-Zarza, A.M., Wright, V.P., 2010b. Calcretes. In: Alonso-Zarza, A.M., Tanner, L.H. (Eds.), Carbonates in Continental Environments: Processes, Facies and Applications. Developments in Sedimentology, 61. Elsevier, Amsterdam, pp. 226–267.

Alonso-Zarza, A.M., Calvo, J.P., García del Cura, M.A., 1992. Palustrine sedimentation and associated features — grainification and pseudomicrokarst — in the Middle Miocene (Intermediate Unit) of the Madrid Basin, Spain. Sedimentary Geology 76, 43–61.

Alonso-Zarza, A.M., Dorado-Valiño, M., Valdeolmillos-Rodríguez, A., Ruiz-Zapata, M.B., 2006. A recent analogue for palustrine carbonate environments: the Quaternary deposits of Las Tablas de Daimiel wetlands, Ciudad Real, Spain. In: Alonso-Zarza, A.M., Tanner, L.H. (Eds.), Paleoenvironmental Record and Applications of Calcretes and Palustrine Carbonates: Geological Society of America, Special Paper, 416, pp. 153–168.

Alonso-Zarza, A.M., Genise, J.F., Verde, M., 2011. Sedimentology, diagenesis and ichnology of Cretaceous and Palaeogene calcretes and palustrine carbonates from Uruguay. Sedimentary Geology 236, 45–61.

Armenteros, I., Daley, B., Garcia, E., 1997. Lacustrine and palustrine facies in the Bembridge Limestone (late Eocene, Hampshire Basin) of the Isle of Wight, southern England. Palaeogeography, Palaeoclimatology, Palaeoecology 128, 111–132.

Blakey, R.C., Gubitosa, R., 1983. Late Triassic paleogeography and depositional history of the Chinle Formation, southern Utah and northern Arizona. In: Reynolds, M.W., Dolly, E.D. (Eds.), Mesozoic Paleogeography of the West-Central United States. Rocky Mountain Section SEPM, Denver, pp. 57–76.

Blakey, R.C., Gubitosa, R., 1984. Controls of sandstone body geometry and architecture in the Chinle Formarion (Upper Triassic), Colorado Plateau. Sedimentary Geology 38, 51–86.

Bohacs, K.M., Carroll, A.R., Neal, J.E., Mankiewicz, P.J., 2000. Lake-basin type, source potential, and hydrocarbon character: an integrated-sequence-stratigraphic – geochemical framework. In: Gierlowski-Kordesch, E.H., Kelts, K.R. (Eds.), Lake Basins through Space and Time: American Association of Petroleum Geologists, Studies in Geology, 46, pp. 3–34.

Bustillo, M.A., 2010. Silicification of continental carbonates. In: Alonso-Zarza, A.M., Tanner, L.H. (Eds.), Carbonates in Continental Environments: Processes, Facies and Applications. Developments in Sedimentology, 62. Elsevier, Amsterdam, pp. 153–179.

Calvo, J.P., Alonso Zarza, A.M., García del Cura, M.A., 1989. Models of Miocene marginal lacustrine sedimentation in response to varied depositional regimes and source areas in the Madrid Basin (central Spain). Palaeogeography, Palaeoclimatology, Palaeoecology 70, 199–214.

Carroll, A.R., Bohacs, K.M., 1999. Stratigraphic classification of ancient lakes: balancing tectonic and climatic controls. Geology 27, 99–102.

Case, E.C., 1916. Further evidence bearing on the age of the red beds in the Rio Grande Valley, New Mexico. Science 77, 708–709.

Cather, S., Osburn, G.R., 2007. Preliminary geologic map of the Cañon Agua Buena quadrangle, Socorro County, New Mexico. New Mexico Bureau of Geology and Mineral Resources, Open-file Geologic Map, p. 146.

Cecil, C.B., 1990. Paleoclimate controls on stratigraphic repetition of chemical and siliciclastic rocks. Geology 18, 533–536.

Clemmensen, L.B., Kent, D.V., Jenkins Jr., F.A., 1998. A Late Triassic lake system in East Greenland: facies, depositional cycles and palaeoclimate. Palaeogeography, Palaeoclimatology, Palaeoecology 140, 135–159.

Cleveland, D.M., Nordt, L.C., Dworkin, S.I., Atchley, S.C., 2008a. Pedogenic carbonate isotopes as evidence for extreme climatic events preceding the Triassic–Jurassic boundary: implications for the biotic crisis? Geological Society of America Bulletin 120, 1408–1415.

Cleveland, D.M., Nordt, L.C., Atchley, S.C., 2008b. Paleosols, trace fossils, and precipitation estimates of the uppermost Triassic strata in northern New Mexico. Palaeogeography, Palaeoclimatology, Palaeoecology 257, 421–444.

Colbert, E.H., 1958. Triassic tetrapod extinction at the end of the Triassic Period. Proceedings of the National Academy of Sciences of the United States of America 44, 973–977.

Davaud, E., Girardclos, S., 2001. Recent freshwater ooids and oncoids from western Lake Geneva (Switzerland): indications of a common organically mediated origin. Journal of Sedimentary Research 71, 423–429.

De Deckker, P., 2002. Ostracod palaeoecology. In: Holmes, J.A., Chivas, A.R. (Eds.), The Ostracoda: Applications in Quaternary Research. : Geophysical Monograph, 131. American Geophysical Union, Washington, pp. 121–134.

De Deckker, P., Forester, R.M., 1988. The use of ostracods to reconstruct continental palaeoenvironmental records. In: De Deckker, P., Colin, J.-P., Peypouquet, J.-P. (Eds.), Ostracoda in the Earth Sciences. Elsevier, Amsterdam, pp. 175–199.

De Wet, C., Yocum, D.A., Mora, C., 1998. Carbonate lakes in closed basins: sensitive indicators of climate and tectonics: an example from the Gettysburg Basin (Triassic), Pennsylvania, USA. In: Stanley, K.W., McCabe, P.J. (Eds.), Role of Eustasy, Climate and Tectonism in Continental Rocks: Society of Economic Paleontologists and Mineralogists Special Publication, 59, pp. 191–209.

Dean, W.E., 1981. Carbonate minerals and organic matter in sediments of modern north temperate hard-water lakes. Society of Economic Paleontologists and Mineralogists. Special Publication 31, 213–231.

Demko, T.M., Dubiel, R.F., Parrish, J.T., 1998. Plant taphonomy in incised valleys: implications for interpreting paleoclimate from fossil plants. Geology 26, 1119–1122.

Dubiel, R.F., 1994. Triassic deposystems, paleogeography, and paleoclimate of the Western Interior. In: Caputo, M.V., Peterson, J.A., Franczyk, K.J. (Eds.), Mesozoic Systems of the Rocky Mountain Region, USA. Rocky Mountain Section SEPM, Denver, Colorado, pp. 133–168.

Dubiel, R.F., Parrish, J.T., Parrish, J.M., Good, S.C., 1991. The Pangaean megamonsoon – evidence from the Upper Triassic Chinle Formation, Colorado Plateau. Palaios 6, 347–370.

Dunagan, S.P., Turner, C.E., 2004. Regional paleohydrologic and paleoclimatic setting of wetland/lacustrine depositional systems in the Morrison Formation (Upper Jurassic), Western Interior, USA. Sedimentary Geology 167, 269–296.

Esteban, M., Klappa, C.F., 1983. Subaerial exposure environments. In: Scholle, P.A., Bebout, D.G., Moore, C.H. (Eds.), Carbonate Depositional Environments: American Association of Petroleum Geologists Memoir, 33, p. 1296.

Ethridge, F.G., Wood, L.J., Schumm, S.A., 1988. Cyclic variables controlling fluvial sequence development: problems and perspectives. In: Schanley, K.J., McCabe, P.J. (Eds.), Relative Role of Eustasy, Climate and Tectonism in Continental Rocks: SEPM, Special Publication, 59, pp. 18–29.

Fielding, C.R., Allen, J.P., Alexander, J., Gibling, M.R., Rygel, M.C., Calder, J.H., 2011. Fluvial Systems and Their Deposits in Hot, Seasonal Semiarid and Subhumid Settings: Modern and Ancient Examples. In: Davidson, S.K., Leieu, S., North, C.P. (Eds.), From River To Rock Record: The Preservation Of Fluvial Sediments And Their Subsequent Interpretation: SEPM, Special Publication, 97, pp. 89–112.

Ford, T.D., Pedley, H.M., 1996. A review of tufa and travertine deposits of the world. Earth-Science Reviews 41, 117–175.

Freytet, P., Plaziat, J.-C., 1982. Continental carbonate sedimentation and pedogenesis – Late Cretaceous and Early Tertiary of southern France. Schweizerbart'sche Verlagsbuchhandlung (N≙gele u. Obermiller). Contributions to Sedimentology 12 (213 pp.).

Freytet, P., Verrecchia, E.P., 2002. Lacustrine and palustrine carbonate petrography: an overview. Journal of Paleolimnology 27, 221–237.

Gierlowski-Kordesch, E.H., 1998. Carbonate deposition in an ephemeral siliciclastic alluvial system: Jurassic Shuttle Meadow Formation, Newark Supergroup, Hartford Basin, USA. Palaeogeography, Palaeoclimatology, Palaeoecology 140, 161–184.

Gierlowski-Kordesch, E.H., 2010. Lacustrine carbonates. In: Alonso-Zarza, A.M., Tanner, L.H. (Eds.), Carbonates in Continental Environments: Processes, Facies and Applications. Developments in Sedimentology, 61. Elsevier, Amsterdam, pp. 1–101.

Gile, L.H., Peterson, F.F., Grossman, R.B., 1966. Morphological and genetic sequences of accumulation in desert soils. Soil Science 100, 347–360.

Guido, D.M., Campbell, K.A., 2011. Jurassic hot spring deposits of the Deseado Massif (Patagonia, Argentina): characteristics and controls on regional distribution. Journal of Volcanology and Geothermal Research 203, 35–47.

Heckert, A. B., 1997. Litho- and biostratigraphy of the lower Chinle Group, east-central Arizona and west-central New Mexico, with a description of a new theropod (Dinosauria: Theropoda) from the Bluewater Creek Formation. M. S. thesis, University of New Mexico, Albuquerque, 278 pp.

Heckert, A.B., 2004. Late Triassic microvertebrates from the lower Chinle Group (Otischalkian-Adamanian: Carnian), southwestern U.S.A., 27. Museum of Natural History and Science, Bulletin, New Mexico, pp. 1–170.

Heckert, A.B., Lucas, S.G., 2002a. The microfauna of the Upper Triassic Ojo Huelos Member, San Pedro Arroyo Formation, central New Mexico, 21. Museum of Natural History and Science Bulletin, New Mexico, pp. 77–85.

Heckert, A.B., Lucas, S.G., 2002b. Lower Chinle Group (Upper Triassic, Carnian) stratigraphy in the Zuni Mountains, west-central New Mexico, 21. Museum of Natural History and Science Bulletin, New Mexico, pp. 51–72.

Heckert, A.B., Ivanov, A., Lucas, S.G., 2007. Dental morphology of the hybodontoid shark Lonchidion humblei Murry from the Upper Triassic Chinle Group, 41. Museum of Natural History and Science Bulletin, New Mexico, pp. 45–48.

Heckert, A.B., Lucas, S.G., Dickinson, W.B., Mortensen, J.K., 2009. New ID-TIMS U-Pb ages for Chinle Group strata (Upper Triassic) in New Mexico and Arizona, correlation to the Newark Supergroup, and implications for the "long Norian. Geological Society of America Abstracts with Programs 41 (7), 123.

Horne, D.J., Cohen, A., Martens, K., 2002. Taxonomy, morphology, and biology of Quaternary and living Ostracoda. In: Holmes, J.A., Chivas, A.R. (Eds.), The Ostracoda: Applications in Quaternary Research. Geophysical Monograph, 131. American Geophysical Union, Washington, p. 5236.

Irmis, R.B., Martz, J.W., Parker, W.G., Nesbitt, S.J., 2010. Re-evaluating the correlation between Late Triassic terrestrial vertebrate biostratigraphy and the GSSP-defined marine stages. Albertiana 38, 40–53.

Janssen, A., Swennen, R., Podoor, N., Keppens, E., 1999. Biological and diagenetic influence in Recent and fossil tufa deposits from Belgium. Sedimentary Geology 126, 75–95.

Jennings, D.S., Lovelace, D.M., Driese, S.G., 2011. Lower Chinle Group (Upper Triassic, Carnian) stratigraphy in the Zuni Mountains, west-central New Mexico. Sedimentary Geology 238, 23–47.

Jones, B., Renaut, R.W., 2010. Calcareous spring deposits in continental settings. In: Alonso-Zarza, A.M., Tanner, L.H. (Eds.), Carbonates in Continental Environments: Processes, Facies and Applications. : Developments in Sedimentology, 61. Elsevier, Amsterdam, pp. 175–225.

Kelts, K., Hsü, K.J., 1978. Freshwater carbonate sedimentation. In: Lerman, A. (Ed.), Lakes: Chemistry, Geology, Physics. Springer, Berlin, pp. 295–323.

Kent, D.V., Olsen, P.E., 1997. Magnetostratigraphy and paleopoles from the Late Triassic Dan River–Danville basin: interbasin correlation of continental sediments and a test of the tectonic coherence of the Newark rift basins in eastern North America. Geological Society of America Bulletin 109, 366–379.

Kent, D.V., Olsen, P.E., 2000. Magnetic polarity stratigraphy and paleolatitude of the Triassic-Jurassic Blomidon Formation in the Fundy basin (Canada): implications for early Mesozoic tropical climate gradients. Earth and Planetary Science Letters 179, 311–324.

Kent, D.V., Tauxe, L., 2005. Corrected Late Triassic latitudes for continents adjacent to the North Atlantic. Science 307, 240–244.

Kozur, H.W., Bachmann, G.H., 2010. The middle Carnian wet intermezzo of the Stuttgart Formation (Schilfsandstein), Germanic Basin. Palaeogeography, Palaeoclimatology, Palaeoecology 290, 107–119.

Kraus, M.J., Middleton, L.T., 1987. Dissected paleotopography and base-level changes in a Triassic fluvial sequence. Geology 15, 18–20.

Lawton, T.F., 1994. Tectonic setting of Mesozoic sedimentary basins. In: Caputo, M.V., Peterson, J.A., Franczyk, K.J. (Eds.), Mesozoic systems of the Rocky Mountain Region, USA. Rocky Mountain Section SEPM, Denver, Colorado, pp. 1–25.

Lucas, S.G., 1991. Triassic stratigraphy, paleontology and correlation, south-central New Mexico, 42. Geological Society, Guidebook, New Mexico, pp. 243–259.

Lucas, S.G., 1993. The Chinle Group: revised stratigraphy and chronology of Upper Triassic nonmarine strata in the western United States. Museum of Northern Arizona, Bulletin 59, 27–50.

Lucas, S.G., 2010. The Triassic timescale based on nonmarine tetrapod biostratigraphy and biochronology. In: Lucas, S.G. (Ed.), The Triassic Timescale: Geological Society, London, Special Publication, 334, pp. 447–500.

Lucas, S.G., Heckert, A.B., 1994. Triassic stratigraphy in the Lucero uplift. Cibola, Valencia and Socorro counties, 45. New Mexico Geological Society, Guidebook, New Mexico, pp. 241–254.

Lucas, S.G., Heckert, A.B., Estep, J.W., Anderson, O.J., 1997. Stratigraphy of the Upper Triassic Chinle Group, Four Corners region, in Mesozoic Geology and Paleontology of the Four Corners Region, 48. Geological Society, Guidebook, New Mexico, pp. 81–108.

Lucas, S.G., Heckert, A.B., Hunt, A.P., 2004. Triassic strata at Carrizo Arroyo. Lucero uplift, central New Mexico, 25. Museum of Natural History and Science Bulletin, New Mexico, pp. 83–87.

Lucas, S.G., Hunt, A.P., Heckert, A.B., Spielmann, J.A., 2007. Global Triassic tetrapod biostratigraphy and biochronology: 2007 status. New Mexico Museum of Natural History and Science Bulletin 41, 229–240.

Lucas, S.G., Tanner, L.H., Kozur, H.W., Weems, R.E., Heckert, A.B., 2012. The Late Triassic timescale: age and correlation of the Carnian-Norian boundary. Earth-Science Reviews 114, 1–18.

Machette, M.N., 1985. Calcic soils of the southwestern United States. In: Weide, D.L. (Ed.), Soils and Quaternary Geology of the Southwest United States: Geological Society of America, Special Paper, 203, pp. 1–21.

Marzolf, J.E., 1994. Reconstruction of the early Mesozoic Cordilleran cratonic margin adjacent to the Colorado Plateau. In: Caputo, M.V., Peterson, J.A., Franczyk, K.J. (Eds.), Mesozoic Systems of the Rocky Mountain Region, USA. Rocky Mountain Section SEPM, Denver, Colorado, pp. 181–215.

Merz-Preiß, M., Riding, R., 1999. Cyanobacterial tufa calcification in two freshwater streams: ambient environment, chemical thresholds and biological processes. Sedimentary Geology 126, 103–124.

Miall, A.D., 1977. A review of the braided-river depositional environment. Earth-Science Reviews 13, 1–62.

Miall, A.D., 1978. Lithofacies types and vertical profile models in braided river deposits, a summary. In: Miall, A.D. (Ed.), Fluvial Sedimentology, Canadian Society of Petroleum Geologists, Memoir, 5, pp. 597–604.

Miall, A.D., 1996. The Geology of Fluvial Deposits. Springer, New York. (582 pp.).

Molina-Garza, R.S., Geissman, J.W., Van der Voo, R., 1995. Paleomagnetism of the Dockum Group (Upper Triassic), northwest Texas: further evidence for the J-1 cusp in the North American apparent polar wander path and implications for the apparent polar wander and Colorado Plateau migration. Tectonics 14, 979–993.

Olsen, P.E., 1986. A 40-million year lake record of Early Mesozoic orbital climate forcing. Science 234, 842–848.

Olsen, P.E., 1997. Stratigraphic record of the early Mesozoic breakup of Pangea in the Laurasia–Gondwana rift system. Annual Review of Earth and Planetary Sciences 25, 337–401.

Olsen, P.E., Kent, D.V., 1996. Milankovitch climate forcing in the tropics of Pangea during the Late Triassic. Palaeogeography, Palaeoclimatology, Palaeoecology 122, 1–26.

Parrish, J.T., 1993. Climate of the supercontinent Pangea. Journal of Geology 101, 215–253.

Peterson, F., 1988. Pennsylvanian to Jurassic eolian transportation systems in the Western United States. Sedimentary Geology 56, 207–260.

Platt, N.H., 1989. Lacustrine carbonates and pedogenesis: sedimentology and origin of palustrine deposits from the Early Cretaceous Rupelo Formation, W Cameros Basin, N Spain. Sedimentology 36, 665–684.

Platt, N.H., 1992. Fresh-water carbonates from the lower Freshwater Molasse (Oligocene, western Switzerland): sedimentology and stable isotopes. Sedimentary Geology 78, 81–99.

Platt, N.H., Wright, V.P., 1991. Lacustrine carbonates: facies models, facies distributions and hydrocarbon aspects. In: Anadón, P., Cabrera, L., Kelts, K. (Eds.), Lacustrine Facies Analysis: International Association of Sedimentologists, Special Publication, 13, pp. 57–74.

Platt, N.H., Wright, V.P., 1992. Palustrine carbonates and the Florida Everglades: towards an exposure index for the fresh-water environment? Journal of Sedimentary Petrology 62, 1058–1071.

Plaziat, J.C., Freytet, P., 1978. Le pseudo-microkasrs pe´dologique: un aspect particulier des pale´o-pe´dogene`ses de´veloppe´ess sur les depots calcaires lacustres dans le tertiaire du Lnaguedoc. Comptes Rendus Academie Science Paris 286, 1661–1664.

Rainey, D.K., Jones, B., 2009. Abiotic versus biotic controls on the development of the Fairmont Hot Springs carbonate deposit, British Columbia, Canada. Sedimentology 56, 1832–1857.

Rogers, R.R., 1994. Nature and origin of through-going discontinuities in nonmarine foreland basin strata, Upper Cretaceous, Montana: Implications for sequence analysis. Geology 22, 1119–1122.

Roghi, G., Gianolla, P., Minarelli, L., Pilati, C., Preto, N., 2010. Palynological correlation of Carnian humid pulses throughout western Tethys. Palaeogeography, Palaeoclimatology, Palaeoecology 290, 89–106.

Sanz, M.E., Alonso-Zarza, A.M., Calvo, J.P., 1995. Carbonate pond deposits related to semi-arid alluvial systems: examples from the Tertiary Madrid Basin, Spain. Sedimentology 42, 437–452.

Schumm, S.A., 1993. River response to baselevel changes: implications for sequence stratigraphy. Journal of Geology 101, 279–294.

Scotese, C.R., 1994. Late Triassic paleogeographic map. In: Klein, G.D. (Ed.), Pangea: Paleoclimate, Tectonics, and Sedimentation During Accretion, Zenith, and Breakup of a Supercontinent: Geological Society of America, Special Paper, 288, p. 7.

Shapiro, R.S., Fricke, H.C., Fox, K., 2009. Dinosaur-bearing oncoids from ephemeral lakes of the Lower Cretaceous Cedar Mountain Formation, Utah. Palaios 24, 51–58.

Simms, M.J., Ruffell, A.H., 1990. Climatic and biotic change in the Late Triassic. Journal of the Geological Society of London 147, 321–327.

Simms, M.J., Ruffell, A.H., Johnson, A.L.A., 1994. Biotic and climatic changes in the Carnian (Triassic) of Europe and adjacent areas. In: Fraser, N.C., Sues, H.D. (Eds.), In the Shadow of the Dinosaurs. Early Mesozoic Tetrapods. Cambridge University Press, pp. 352–365.

Spielmann, J.A., Lucas, S.G., 2009. Triassic stratigraphy and biostratigraphy in Socorro County, 60. New Mexico Geological Society, Guidebook, New Mexico, pp. 213–225.

Stewart, J.H., Poole, F.G., Wilson, R.F., 1972. Stratigraphy and Origin of the Chinle Formation and Related Upper Triassic Strata in the Colorado Plateau Region. U.S. Geological Survey, Professional Paper, 690. 336 pp.

Stewart, J.H., Anderson, T.H., Haxel, G.B., Silver, L.T., Wright, J.E., 1986. Late Triassic paleogeography of the southern Cordillera: the problem of a source for voluminous volcanic detritus in the Chinle Formation of the Colorado Plateau region. Geology 14, 567–570.

Talbot, M.R., Holm, K., Williams, M.A.J., 1994. Sedimentation in low-gradient desert margin systems: A comparison of the Late Triassic of northwest Somerset (England) and the late Quaternary of east-central Australia. In: Rosen, M.R. (Ed.), Paleoclimate and Basin Evolution of Playa Systems: Geological Society of America, Special Paper, 289, pp. 97–117.

Tandon, S.K., Narayan, D., 1981. Calcrete conglomerate, case-hardened conglomerate and cornstone: a comparative account of pedogenic and non-pedogenic carbonates from the continental Siwalik Group, Punjab, India. Sedimentology 28, 353–367.

Tanner, L.H., 2000. Palustrine-lacustrine and alluvial facies of the (Norian) Owl Rock Formation (Chinle Group), Four Corners Region, southwestern U.S.A.: implications for Late Triassic paleoclimate. Journal of Sedimentary Research 70, 1280–1289.

Tanner, L.H., 2003. Pedogenic features of the Chinle Group, Four Corners region; Evidence of Late Triassic aridification. New Mexico Geological Society, Guidebook 54th Field Conference, pp. 269–280.

Tanner, L.H., 2010. Terrestrial carbonates as indicators of palaeoclimate. In: Alonsa-Zarza, A.M., Tanner, L.H. (Eds.), Carbonates in Continental Settings: Geochemistry, Diagenesis and Applications. Developments in Sedimentology, 62. Elsevier, Amsterdam, pp. 179–214.

Tanner, L.H., Lucas, S.G., 2006. Calcretes of the Upper Triassic Chinle Group, Four Corners region, southwestern U.S.A.: climatic implications. In: Alonso-Zarza, A.M., Tanner, L.H. (Eds.), Paleoenvironmental Record and Applications of Calcretes and Palustrine Carbonates: Geological Society of America, Special Paper, 416, pp. 53–74.

Tanner, L.H., Lucas, S.G., 2007. Origin of sandstone casts in the Upper Triassic Zuni Mountains Formation, Fort Wingate, 40. New Mexico Museum of Natural History and Science Bulletin, New Mexico, pp. 209–214.

Tanner, L.H., Hubert, J.F., Coffey, B.P., McInerney, D.P., 2001. Stability of atmospheric CO_2 levels across the Triassic/Jurassic boundary. Nature 411, 675–677.
Tanner, L.H., Lucas, S.G., Chapman, M.G., 2004. Assessing the record and causes of Late Triassic extinctions. Earth-Science Reviews 65, 103–139.
Tucker, M.E., Benton, M.J., 1982. Triassic environments, climates, and reptile evolution. Palaeogeography, Palaeoclimatology, Palaeoecology 40, 361–379.
Tucker, M.E., Wright, V.P., 1990. Carbonate Sedimentology. Blackwell Scientific Publications, Oxford. (482 pp.).
Verrechia, E.P., 2007. Lacustrine and palustrine geochemical sediments. In: Nash, D.J., McLaren, S.J. (Eds.), Geochemical Sediments and Landscapes. Blackwell, Malden, Massachusetts, pp. 298–329.
Wright, V.P., 1990. Syngenetic formation of grainstones and pisolites from fenestral carbonates in peritidal settings: discussion. Journal of Sedimentary Petrology 60, 309–310.
Wright, V.P., 2007. Calcrete. In: Nash, D.J., McLaren, S.J. (Eds.), Geochemical Sediments and Landscapes. Blackwell, Malden, Massachusetts, pp. 10–45.
Zhou, J., Chafetz, H., 2009. Biogenic caliches in Texas: the role of organisms and effect of climate. Sedimentary Geology 222, 207–225.